Available online at www.CivileJournal.org

Civil Engineering Journal

(E-ISSN: 2476-3055; ISSN: 2676-6957)

Vol. 12, No. 01, January, 2026

Shear Behavior of Small-Scale Continuous Hidden Beams Using Tied and Spiral Stirrups

Mostafa Ahmed [1], Januarti J. Ekaputri [2*], Hany Abdalla [1], Ahmed Elgamal [3], Ahmed Youssef [1*]

[1] *Department of Structural Engineering, Faculty of Engineering, Cairo University, Cairo 12613, Egypt.*

[2] *Department of Civil Engineering, Faculty of Civil, Planning and Geo Engineering, Institut Teknologi Sepuluh Nopember, Kampus ITS, Sukolilo, Surabaya 60111, Indonesia.*

[3] *Structural Engineering Department, Faculty of Engineering, Damietta University, New Damietta 34517, Egypt.*

Received 16 November 2025; Revised 24 December 2025; Accepted 29 December 2025; Published 01 January 2026

Abstract

Hidden beams in reinforced concrete (RC) structures are widely used to meet architectural requirements; however, their reduced effective depth limits shear capacity. This study investigates the shear behavior of hidden beams reinforced with innovative rectangular staggered continuous spiral stirrups, addressing the absence of design guidelines for such reinforcement systems. Nine one-eighth-scale continuous beams were tested under two-point loading, with mortar used to reduce scale effects. The influence of the number, geometry, and configuration of spiral reinforcement was investigated. Both conventional and spiral stirrups significantly improved shear performance compared to the reference beam without transverse reinforcement (HB9-No). Beams with normal stirrups (HB1-N20, HB2-N30, HB3-N40, HB4-N50) increased shear capacity by 115%, 82%, 23%, and 4%, while spiral stirrup beams (HB1-S20, HB2-S30, HB3-S40, HB4-S50) achieved corresponding increases of 174%, 144%, 73%, and 27%, respectively. Overall, spiral reinforcement enhanced shear capacity and energy dissipation by approximately 30% and 46%, respectively, compared with conventional stirrups. Prototype capacities estimated using scaling relationships were compared with international design codes, which were found to be conservative. The findings demonstrate the effectiveness of spiral stirrups in improving shear strength and ductility and emphasize the need to include their contribution in future shear design equations for hidden beams.

Keywords: Scale Down Modelling (SDM); Shear Resistance; Reinforced Concrete; Hidden Beams; Stirrups; Tied; Spiral.

1. Introduction

Hidden beams, or wide reinforced concrete (RC) beams, are found to provide for the passage of multiple services beneath RC floors using a comparatively small depth, resulting in a larger story clear height and further labor and material cost savings [1]. According to Conforti et al. (2015), numerous global building codes define hidden beams as structural elements with widths exceeding twice their corresponding depths [2]. Nevertheless, these structural members exhibit diminished shear strength and reduced ductility due to their limited depth [3, 4]. It is critical to avoid shear failure in structures by increasing their ductility, which can lead to catastrophic failure. It is this mode of failure that necessitates the development of more efficient methods for designing shear beams. A continuous spiral form can replace the conventional stirrups, thereby improving concrete confinement and structural performance [5].

* Corresponding author: januarti@ce.its.ac.id; ahmedyoussef@cu.edu.eg

https://doi.org/10.28991/CEJ-2026-012-01-06

Due to its excellent ductile properties, particularly in seismic conditions, this form of arrangement is used chiefly in R.C. columns. Spiral arrangements would not be so satisfactory in R.C. beams owing to the restrictive conditions in design and the state of knowledge as to the deficiency of experimental work in this direction. A multitude of experimental and analytical investigations have examined improvements in concrete characteristics under confinement [6]. Multiple studies have been conducted on this topic. For example, Shatarat et al. (2016) [7] investigated 28 R.C. beams subjected to four-point loading with spiral stirrups as transverse reinforcement. Three different spacings and two shear-arm ratios were studied, and five different angles of inclination of stirrups were investigated. To enhance the shear strength and ductility of the beams, Shatarat recommended applying the ACI design shear formula to implement spiral ties. In a similar investigation, Joshy & Faisal (2017) [8] examined 12 reinforced concrete beams under a four-point load using spiral stirrups in self-compacting concrete (S.C.C.), with various tie spacings as the variable. The results indicate that continuous spiral ties deliver better performance than single ties in terms of construction efficiency, increased ductility, and increased shear strength. Furthermore, the use of self-compacted concrete (S.C.C.) appears to lend itself to better development of critical cracks.

An experimental investigation by Iyengar et al. (1972) [9] examined the stress–strain characteristics of confined concrete. The authors not only investigated the behavior of reinforced concrete frames but also tested continuous and supported reinforced concrete beams. From this work, an index was established to quantify the amount of confinement provided by the transverse reinforcement. In a subsequent and innovative study, Mander et al. (1988) [10] introduced a stress–strain model to characterize the behavior of concrete under uniaxial compression when confined by transverse reinforcement. Mander's study demonstrated that the ultimate compressive strain of confined concrete can be estimated by evaluating the work done on both the confined concrete and the longitudinal steel reinforcement. The experimental program included thirty-one short RC columns with varying cross-sectional shapes and reinforcement configurations, and the proposed stress–strain model was validated using these experimental results. Additionally, Hua & Wu (2018) [11] conducted an experimental investigation on eleven RC beams to determine the shear strength contributions of both stirrups and concrete. The study concluded that key structural variables included the type of transverse reinforcement (plain round or deformed bars) and variations in the a/d ratio.

Meghana & Vedic (2018) [12] assessed the strength of reinforced concrete beams of different configurations of continuous spiral stirrup. The results have suggested that continuous spirals are a significant benefit in terms of cost savings. Kumar & Sreevalli (2020) [13] studied the impact of confinement steel bars on the bending behavior of reinforced concrete beams under cyclic loads. Some of the confinement patterns studied included separate ties, inclined ties, rectangular spirals, and lacing. Based on the study results, the angled and laced ties are more ductile than the separate ties and the rectangular spirals. Dewi et al. (2020) [14] conducted experimental investigations on nine reinforced concrete beams with circular cross sections regarding their shear strength. The parameters examined are the type of stirrups employed and the extent of the reinforcement. The specimen consists of six without ties, three with conventional tying methods, and three with a spiral stirrup system. Experimental investigations indicate that specimens without ties failed in shear, whereas specimens with spiral stirrups exhibited increased ductility in developing plastic hinges. A research program executed by Karayannis & Chalioris (2013) [15] examined eight critical shear-reinforced concrete beams under monotonic load. The results of their investigation showed that the use of spiral reinforcement has a substantial effect on the flexural and shear strength of the tested experimental beams.

The significance of the spiral ties system in locations near probable plastic hinges of reinforced concrete beams cracked under high cyclic flexure was experimentally examined by Jaafar (2008) [16]. The results showed that by using an overlapping spiral tie system, the shear strength of the reinforced concrete beams is increased under cyclic load due to its confining influence. Azimi et al. (2016) [5] developed a spiral shear reinforcement configuration for reinforced concrete beam-column joints exposed to cyclic loading. Their study indicated that continuous twisted reinforcement arrangements exhibited improved seismic response and a superior distribution of cracks relative to traditional rectangular spiral and shear reinforcement systems. Jaafar (2013) [17] analyzed the behavior of reinforced concrete beams under combined shear forces and moments, considering spiral lateral reinforcement, analytically. To assess the shear resistance provided by the spiral lateral reinforcement in the beams under study, the research proposed a simplified sectional model.

Due to their intrinsically brittle failure characteristics, over-reinforced beams are typically prohibited by building codes. However, their performance when spiral reinforcement is used in the compression zone has been well studied by Mohamed (2018) [18] and Tee et al. (2018) [19]. Mohamed (2018) [18] studied the effect of two types of transverse reinforcement, the spiral and rectangular tie types, on the ductility of reinforced concrete beams experimentally. The results show clearly that placing one of these reinforcement types in the beam's compression zone will considerably increase ductility. The test results also show that the beams with spiral ties exhibited deflections much higher than those of the beams with rectangular tie-type reinforcement. The other thing discovered in these tests was that confinement by means of spiral or rectangular stirrups in the compression zone of the reinforced concrete beams permits a change in the type of failure from a brittle mechanism to a ductile mechanism.

Abdelkhaliq & Hilal (2017) [20] conducted an experimental investigation on a total of 12 reduced-scale RC beams subjected to four-point flexural loading to failure. The investigation examined the effects of the longitudinal

reinforcement ratios, stirrup spacing, and the nature of confinement on the structural behavior of the beams. The observations obtained in the experiments were confirmed by an analytical method based on a model suggested by Mander (1988a). This model was developed to accommodate the loading capacities of RC beams with unconventional types of lateral reinforcement. Beams with stirrups fitted in the compression zones exhibited much higher degrees of total deformation, strain, and ductility than those without such confinement. The results also implied that, in flexural members confined in the compression zone, the load-carrying capacity increases by 20 to 30% compared to beams where such confinements were neglected.

Tee et al. (2018) [19] conducted experimental studies on the shear strength, flexural capacity, and deflection behavior of over-reinforced concrete beams using double spiral and double square-shaped steel reinforcement as confining elements in the compression regions. The study used four-point bending tests to evaluate seven reinforced concrete beam specimens with varying longitudinal-to-transverse reinforcement ratios. In addition, eight concrete cylinders reinforced with spirals were tested as part of the experimental program. According to the findings, the confined cylinders' compressive strength was 1.34 to 2.22 times that of similar unconfined specimens.

Li et al. (2025) [21] investigated the shear behavior of eight steel fiber-reinforced concrete (SFRC) beams with glass fiber-reinforced polymer (GFRP) stirrups (GFRP-R-SFRC) under four-point loading. The study considered the effects of steel fiber volume fraction (Vf) and shear span ratio (λ) on failure mode, mid-span deflection, crack width, SFRC and rebar strains, and shear capacity. Increasing λ from 1.5 to 3.0 led to sequential failure modes: diagonal compression, shear compression, and diagonal tension. Incorporating 1.5% steel fibers reduced maximum deflection, crack width, and strains, indicating improved post-cracking stiffness, and increased the strain and utilization of GFRP stirrups due to crack-bridging. Shear capacity increased by 25.6% with Vf from 0% to 1.5%, while increasing λ decreased shear capacity as the failure mode shifted from shear- to flexure-dominated. A modified computational model that incorporates the effects of steel fibers accurately predicted shear capacity and showed good agreement with experimental results.

Yu et al. (2024) [22] explored the shear performance of reinforced concrete beams strengthened with high-toughness resin concrete steel mesh (HTRCS) composites through four-point bending tests on two standard and six HTRCS-reinforced beams. Results showed that HTRCS increased shear capacity by 10–65%, with stiffness significantly influenced by HTRCS thickness, shear–span ratio, and concrete strength, the latter having the most significant effect. The findings provide a theoretical basis for the application of HTRCS in reinforced concrete structures.

He et al. (2025) [23] experimentally investigated the shear performance of concrete beams reinforced with glass FRP (GFRP)-steel hybrid stirrups. Nine hybrid stirrup-reinforced beams and one conventional steel-reinforced beam were tested under four-point bending, with variations in concrete strength (C35, C40, C50), shear span ratio (1, 2, 2.5, and 3), and stirrup spacing (100, 130, 10, and 190 mm). Results showed that hybrid stirrup beams exhibited ductile shear-compression (SC) failure and higher shear strength than conventional steel-reinforced beams. Shear strength was positively correlated with concrete strength and stirrup ratio, but decreased with increasing shear span ratio. Finite element models in ABAQUS accurately reproduced load-displacement behavior. Using the verified model, a database of 144 specimens was generated to evaluate the code equations and four machine-learning (ML) algorithms. Code equations were conservative and scattered, whereas ML algorithms demonstrated superior predictive performance for shear strength.

Abdullah et al. (2024) [24] conducted a three-dimensional evaluation of crack development to investigate the shear failure mechanism of RC beams with two, three, and four vertical stirrup legs, using three-point bending tests with comparable stirrup contributions. The study analyzed load-displacement behavior, surface and internal crack propagation, stirrup and concrete strains, and shear resistance components. Results indicated that two equally spaced internal vertical stirrup legs, combined with conventional closely spaced stirrups, effectively restricted internal crack initiation and propagation to the side surfaces, thereby influencing the beam's shear strength.

Ghalla et al. (2025) [25] examined the effectiveness of external post-tensioning in enhancing the behavior of RC beams without shear reinforcement using experimental and numerical approaches. Fourteen beams were tested to assess the influence of post-tensioning force levels and bar inclination angles. Results showed that post-tensioning improved failure behavior, transforming brittle failure into ductile and promoting more favorable crack distribution. Beams exhibited increased cracking and ultimate loads, with greater improvements at higher force levels and for inclined post-tensioning at 75°, 60°, and 45°, with 60° providing the most significant enhancement in strength and stiffness. The system also increased absorbed energy.

Gouda et al. (2025) [26] studied the combined shear and torsional behavior of reinforced concrete (RC) beams reinforced with continuous glass-fiber reinforced polymer (GFRP) spiral stirrups. Six RC beams (3000 × 200 × 400 mm) were tested to examine the effects of transverse reinforcement type (GFRP spirals vs. tie stirrups) and reinforcement ratio. Beams with GFRP spirals or tie stirrups failed due to widening diagonal cracks and rupture of GFRP bars at bends, whereas the control beam failed by concrete splitting. Results showed that reducing the spacing of GFRP spirals significantly improved shear and torsional capacities. Experimental findings were compared with existing design codes and a newly proposed space truss-based predictive model.

Chen et al. (2025) [27] investigated the shear performance of circular concrete members reinforced with an innovative fiber-reinforced polymer (FRP) stirrup. The study examined the effects of stirrup type and ratio on shear behavior. Results showed that FRP grid spiral-reinforced concrete cylinders (FSRCC) exhibited 16.2% higher shear strength than FRP hoop-reinforced cylinders (FHRCC), with failure mode shifting from shear tension to flexure compression. Increasing the stirrup ratio from 0.32% to 0.72% led to a maximum shear strength increase of 26.0%. The CSA S806–12 code accurately predicted FSRCC shear strength. A finite element model in ABAQUS/Explicit, incorporating FRP–concrete bond-slip behavior, simulated the shear response, and parametric analysis indicated that the longitudinal reinforcement ratio was the most influential factor for enhancing shear capacity.

A study on the effect of spiral reinforcement on concrete mechanical properties was conducted by Elansary et al. (2022) [28], who tested 18 cylindrical specimens under axial compression and splitting tension, incorporating one, two, or three overlapping spirals, and compared them with unconfined controls. Their program also included nine RC beams tested under four-point bending to evaluate shear enhancement from different spiral configurations relative to a conventionally stirrup-reinforced reference beam, along with two additional beams without lateral reinforcement to assess dowel action. The results showed that the beam with two spirals at 100 mm spacing achieved the same failure load as the reference beam despite having 47% less shear reinforcement. Beams with two and three spirals at 200 mm spacing also contained less reinforcement but failed at loads 14% and 9% lower than the reference beam, respectively.

Youssef et al. (2024) [29] and Mahmoud et al. (2022) [30] examined the influence of different transverse reinforcement (RFT) configurations on the torsional and shear performance of miniature RC beams. The program tested 22 scaled beams in shear (800 × 50 × 75 mm) and torsion (900 × 50 × 75 mm), grouped according to four RFT patterns: stirrup spacing for closed stirrups, stirrup spacing for staggered spirals, shear-arm ratio for closed stirrups, and shear-arm ratio for staggered spirals. Using validated scaling techniques, the study compared conventional stirrups with rectangular staggered continuous spirals. The results indicated that staggered spirals markedly increased peak shear capacity due to improved confinement, while design codes EC2-04, ECP 203–20, and ACI 318–19 provided conservative yet acceptable estimates of shear strength.

Experimental investigations of projected or wide beams and other structural elements, many of which utilize scale-down modeling techniques, have been compared in several studies. These comparisons assess the accuracy and reliability of different modeling approaches for predicting structural performance. Mander (1988) [10], Elbasha & Hadi (2005) [31], Tee et al. (2018) [19], Ziara et al. (2000) [32], Mosley et al. (1999) [33], Ahmed et al. (2007) [34], Priastiwi et al. (2014) [35] Priastiwi et al. (2015) [36], Jang et al. (2009) [37], Ahmed, A et al. (2021) [38], Mohammed et al. (2021) [39], Mohammed & Maekawa (2012) [40], Abdelaal & Youssef (2023) [41], and Youssef et al. (2023) [42], in addition to the shear resistance estimated using the equations provided in both the current and previous editions of the ACI 318–19 code (ACI Committee, 2019) [43].

$$V_n = V_c + V_s \tag{1}$$

$$V_c = 0.17\lambda\sqrt{f_c'}b_w d \tag{2}$$

$$V_s = A_v f_{yv}\, d/s \tag{3}$$

where V_n represents the overall nominal shear strength, while V_s and V_c designate the nominal shear strength contributions from stirrups and concrete, respectively. The modification factor λ equals 1 for normal-weight concrete. The stirrup area, yield stress, adequate beam depth, and stirrup spacing are designated by A_v, f_{yv}, d, and s, respectively.

Although spiral reinforcement has demonstrated favourable confinement and shear-enhancing characteristics in various RC elements, its application in wide hidden beams has not been extensively studied, and current design codes do not account for the shear contribution of spiral stirrups. Furthermore, no previous research has investigated rectangular staggered continuous spiral configurations, which may optimize confinement efficiency and improve shear behavior in hidden beams.

In summary, based on the reviewed literature, hidden beams tend to exhibit relatively weak structural performance due to their limited depth. At the same time, previous studies have shown that spiral stirrups can significantly enhance the shear behavior and crack resistance of structural elements. However, research on the application of spiral reinforcement in wide hidden beams remains limited, and existing design guidelines do not account for their shear contribution. Therefore, the current study introduces a novel stirrup configuration using rectangular staggered continuous spiral stirrups to improve the shear capacity and deformation characteristics of hidden beams. The proposed arrangement aims to optimize crack control, enhance energy dissipation, and overcome the inherent shear limitations of hidden beams. In this paper, nine one-eighth-scale beams were experimentally tested under two-point loading to examine the influence of stirrup type, spacing, and configuration. The experimental results are presented and discussed in detail,

followed by a comparison between the scaled prototype capacities and predictions from various international design codes to assess their conservatism. The present manuscript design recommendation of RC specimens could be summarized and illustrated in the next flowchart, as shown in Figure 1.

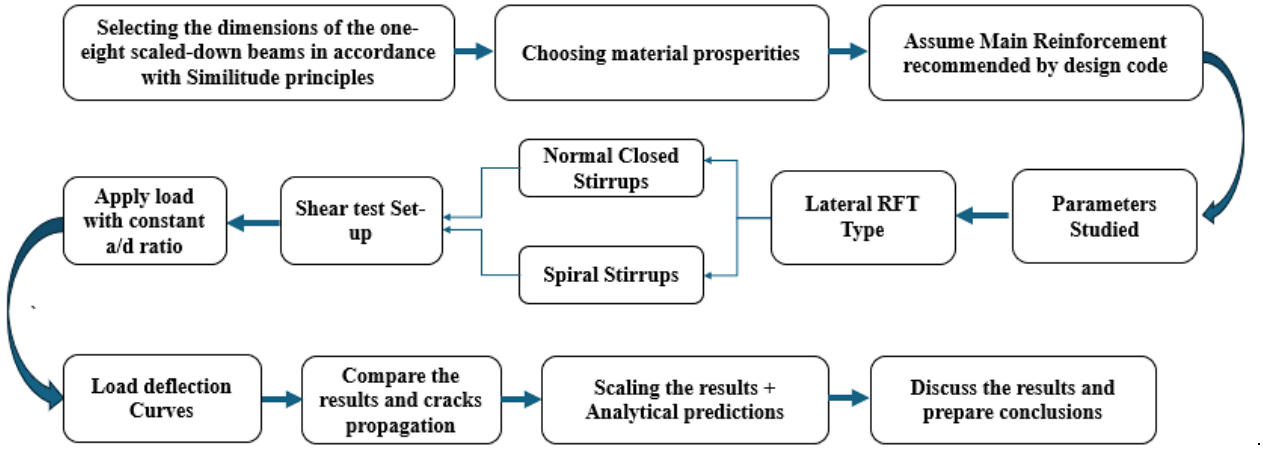

Figure 1. The flowchart research methodology

This study investigates the shear behavior of small-scale beams that are reinforced with rectangular continuous spiral stirrups. The experiment used nine one-eighth-scale beams with a rectangular cross-section. The structural parameters examined included (1) the arrangement of stirrups, with particular emphasis on comparing conventional rectangular stirrups to staggered rectangular continuous spiral stirrups, and (2) stirrup spacing set at 20, 30, 40, and 50 mm. The shear arm ratio was 2.7 across all specimens. The concrete properties and longitudinal reinforcing configuration used to fabricate each specimen were identical. The scaled-down modeling approach used in this study has been extensively studied in the literature and has been partially verified for investigating shear-related phenomena. This work investigates the shear behavior of spirally reinforced concrete (RC) wide beams under monotonic loading, motivated by the paucity of design standards and research on this topic. The study's three main goals are to (1) evaluate how well spiral stirrups improve shear behavior, with a focus on load-deflection response and crack development; (2) examine how RC wide beams reinforced with spirals behave in comparison to those reinforced with conventional closed stirrups; and (3) determine whether the design reinforced concrete code equations are appropriate for estimating the shear capacity of spirally reinforced wide beams.

2. Experimental Program

2.1. Test Setup

The experimental program was conducted in the Concrete Research Modeling Laboratory at Cairo University. A load cell with a capacity of 300 kN was used to measure the applied loads. Load distribution to the specimens was achieved using a spreader beam supported by two rollers, as illustrated in Figure 2. The investigated structural parameters comprised tie spacing and stirrup configurations. Loading was applied through a hydraulic jack to a steel plate, subsequently transferred to the spreader beam, and then to the specimen. Mid-span deflections of each specimen were recorded using two linear variable displacement transducers (LVDTs). To assess the shear capacity of the reinforced concrete beams, the tests' incremental load levels, crack formation, and failure mechanisms were recorded, and the outcomes were analyzed.

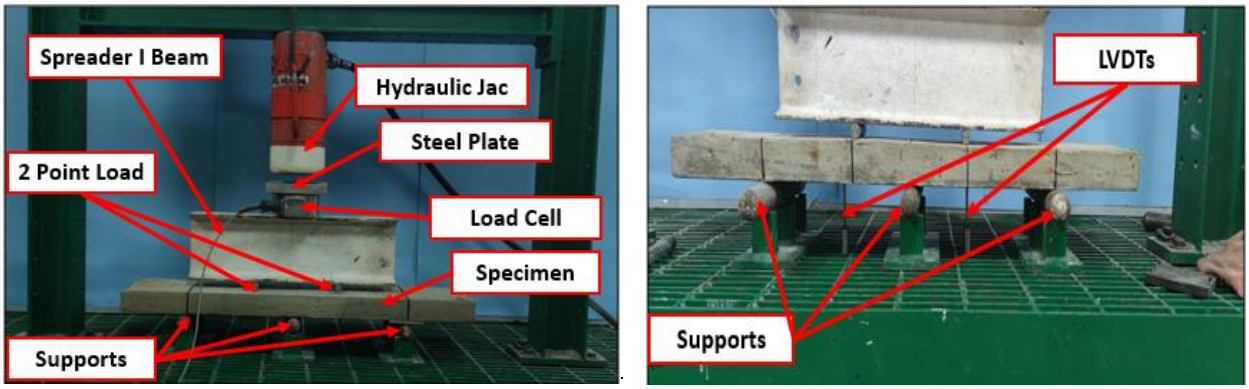

Figure 2. The setup for the shear test

2.2. Specimen Details

The experimental investigation examined the shear behavior of the scaled-down beams subjected to monotonous loads. The study investigated nine reinforced concrete (RC) beams with a rectangular cross-section of 175 × 40 mm. Each beam had a total length of 800 mm, with an effective span of 500 mm for testing. The beams were reinforced longitudinally with 8ϕ4 at the bottom and 8ϕ3 at the top. To prevent anchorage slippage, the reinforcement bars at both the upper and lower sections of all beams were extended beyond the supports. Figures 3 and 4 illustrate the geometry and reinforcement details of the miniature beams, which were equipped with either normal or staggered spiral stirrups. The parameters investigated in this study included stirrup spacing and stirrup configuration. Table 1 summarizes the parameters of the models studied.

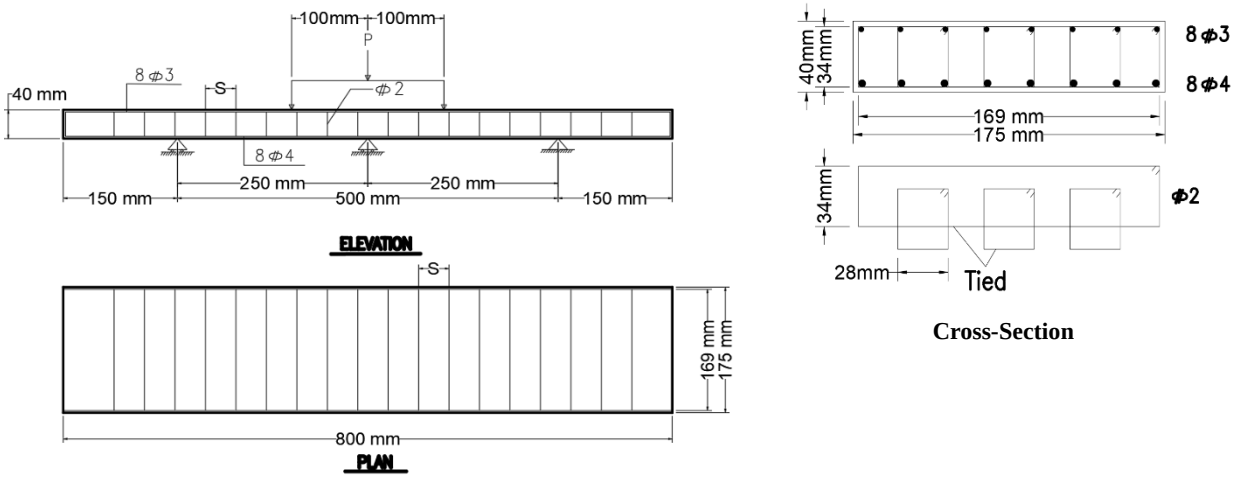

Figure 3. The geometry of the miniature reinforced with tied stirrups

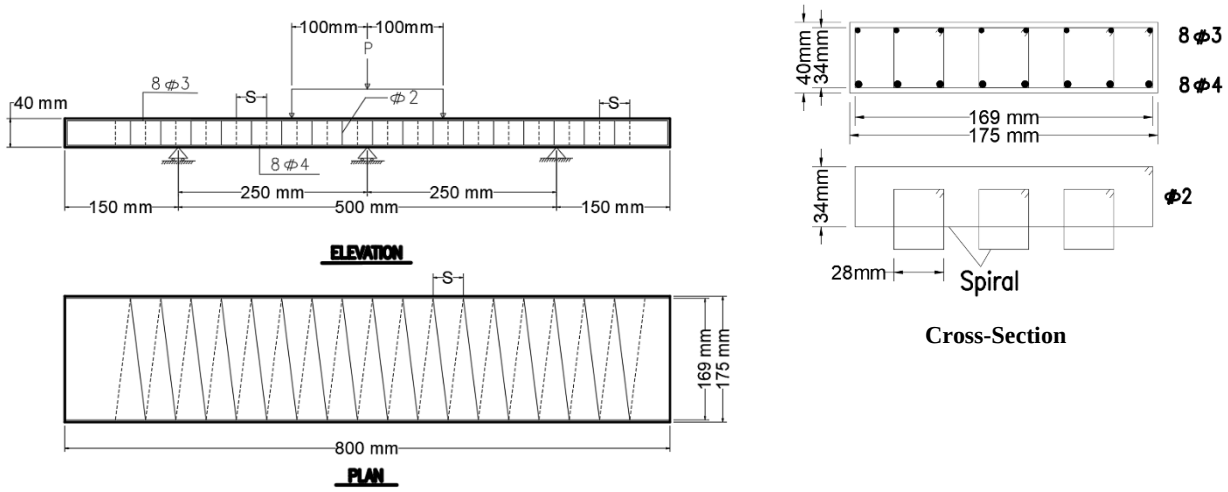

Figure 4. The geometry of the miniature reinforced with spiral stirrups

Table 1. The parameters studied for miniatures

Specimen	Stirrup spacing (mm)	Shear span arm ratio (a/d)	Type of Transverse RFT
HB1-N20	20	2.7	Normal Stirrups
HB2-N30	30	2.7	Normal Stirrups
HB3-N40	40	2.7	Normal Stirrups
HB4-N50	50	2.7	Normal Stirrups
HB5-S20	20	2.7	Spiral Stirrups
HB6-S30	30	2.7	Spiral Stirrups
HB7-S40	40	2.7	Spiral Stirrups
HB8-S50	50	2.7	Spiral Stirrups
HB9-No	No Stirrups	2.7	-

2.3. Casting Procedure

The materials required for the casting process—including sand, cement, water, and performance-enhancing additives—were systematically prepared. The fine materials, both sand and cement, were then sieved, and the required quantities were weighed. The wooden formwork was constructed to the specified design dimensions. The reinforcement cage had been prepared in advance and was subsequently placed inside the wooden formwork after a thin layer of oil was applied to facilitate the removal of the samples post-casting. The mixture was then poured after the mixing phase was complete. Twenty-four hours after casting, the samples were demolded and placed in curing tanks, where they were scheduled for testing after 28 days.

2.4. Material Properties

The normal-weight concrete, designated C40, contained only fine aggregate (sand) with a maximum particle size of 4.75 mm. For the small-scale RC hidden beam specimens, three standard cubes (150 × 150 × 150 mm) and three smaller cubes (75 × 75 × 75 mm) were prepared for each mortar mix before casting. The small-scale RC hidden-beam specimens and the mortar cubes were tested on the same day after curing. Because of the specimens' smaller size, non-commercial reinforcing was used. The mortar was mixed with Addicrete BV to improve workability. As a water-reducing plasticizer, this addition complies with ASTM C 494 Type A, EN 934–2, and ES 1899–1 specifications. Standard dosages range from 0.15% to 0.3% of cement weight, or roughly 0.5–1 kg/m³ of concrete, or 0.25–0.5 kg per 100 liters of water. Table 2 summarizes the final ingredients used across all specimens, while Figure 5 illustrates the grading of fine aggregate. Table 3 lists the precise mechanical characteristics of rebar reinforcement. Additionally, Figures 6 to 8 depict the stress-strain curves corresponding to rebar diameters of 1.9 mm, 3 mm, and 4 mm, respectively. Figure 9 presents the details of the miniature's reinforcement (RFT).

Table 2. Mortar final ingredient specimens by weight

Sand (kg)	Cement (kg)	Water (kg)	Additives ADDICRETE BV (gm/lit of mixing water)
1000	600	240	0.005

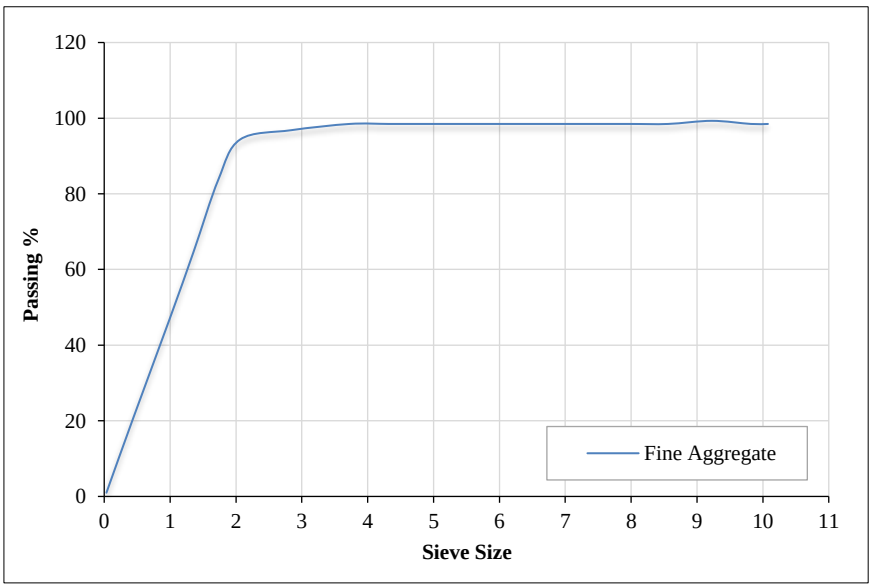

Figure 5. Fine Aggregate Grading

Table 3. Mechanical properties of rebar reinforcement

Diameter (mm)	Area (mm²)	Young's Modulus	Yield stress (N/mm²)	Ultimate Stress (N/mm²)
4.0	12.57		691	768
3.0	7.10	85600 MPa	740	918
1.9	2.83		744	828

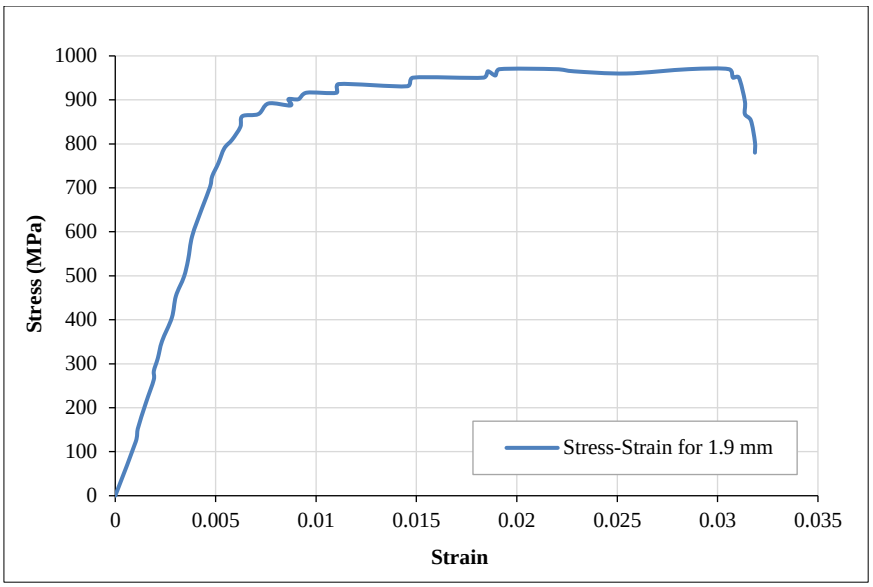

Figure 6. Stress-Strain Curve for 1.9 mm diameter

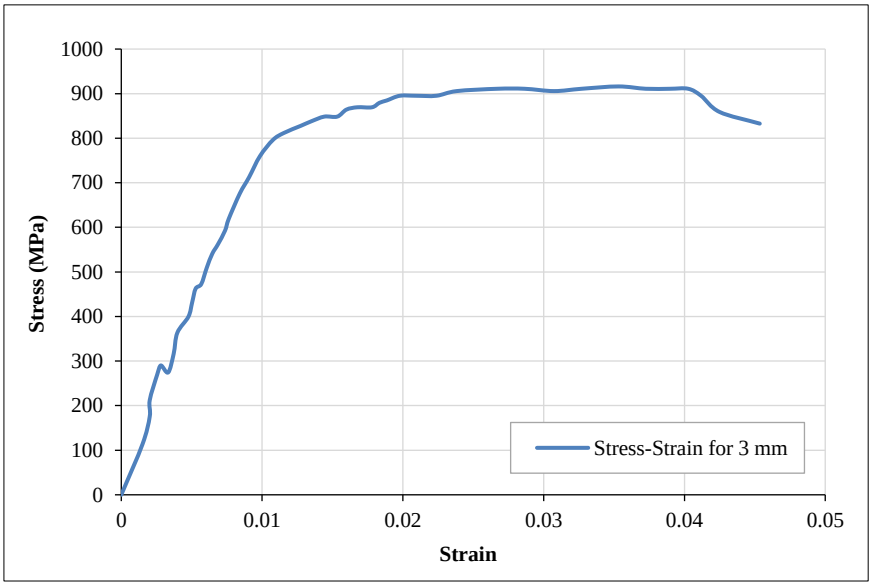

Figure 7. Stress-Strain Curve for 3 mm diameter

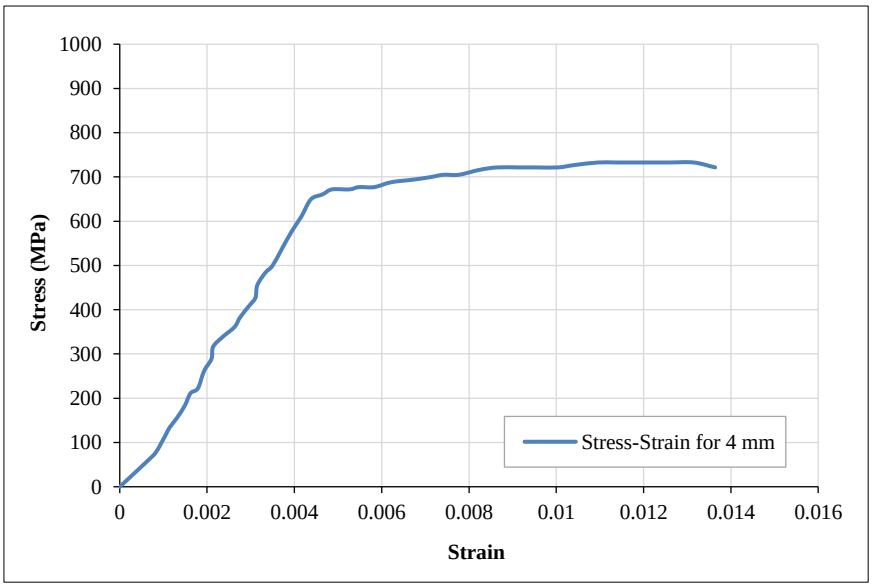

Figure 8. Stress-Strain Curve for 4 mm diameter

Figure 9. the miniature's RFT

3. Discussions of Experimental Results

The experimental program focused on evaluating the shear behavior of hidden RC beams reinforced with either conventional stirrups or staggered rectangular spiral stirrups. The shear load-deflection curve, crack propagation, and energy dissipation capacity of each beam are among the findings from testing (RC) specimens.

3.1. Shear Load-deflection Curve for Diverse Stirrup Spacing

Figures 10 to 23 present the shear load–deflection responses for specimens reinforced with conventional normal stirrups and continuous rectangular spiral stirrups, with stirrup spacings of 20, 30, 40, and 50 mm, maintaining a constant a/d ratio of 2.7. A small a/d ratio of 2.7 was selected for all beams to focus on the effects of lateral reinforcement, noting that smaller a/d ratios typically lead to pure shear failure, while higher a/d ratios result in flexural-shear failure. Firstly, to serve as a reference in the comparative analysis of results, and due to the Egyptian code's disregard for the contribution of stirrups to the shear resistance of hidden beams, a reference specimen (HB9), reinforced only with longitudinal bars without any transverse reinforcement, was included to highlight the critical role of shear reinforcement in hidden beams. HB9 exhibited a sudden brittle failure with a maximum load of 14.03 kN and a deflection of 1.88 mm, confirming the necessity of transverse reinforcement for enhancing ductility and preventing premature shear collapse. In contrast, specimens reinforced with conventional stirrups exhibited improved shear capacity and deformation capacity. Specimen HB1, with 20 mm stirrup spacing, reached a peak load of 30.18 kN at a deflection of 3.60 mm. The inclusion of continuous staggered rectangular spiral stirrups further enhanced performance. Specimen HB5, with spiral stirrups, achieved the highest shear capacity of 38.50 kN with a deflection of 4.02 mm, reflecting an approximate 27.5% increase in peak load compared to conventional stirrups.

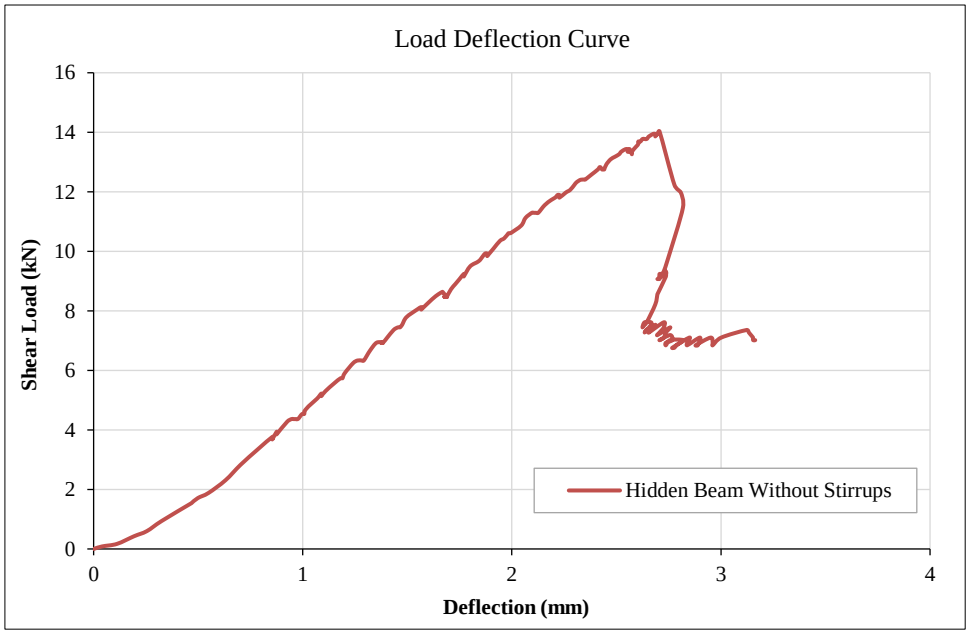

Figure 10. Load Versus Deflection Curve of Specimen without Stirrups

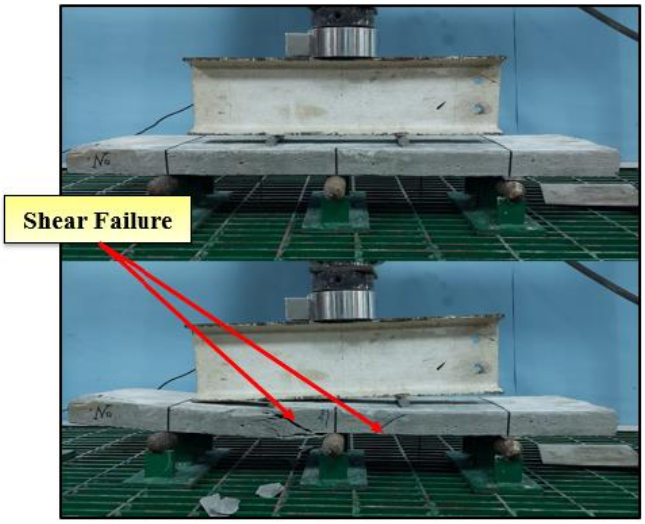

Figure 11. Loading of Specimen without Stirrups

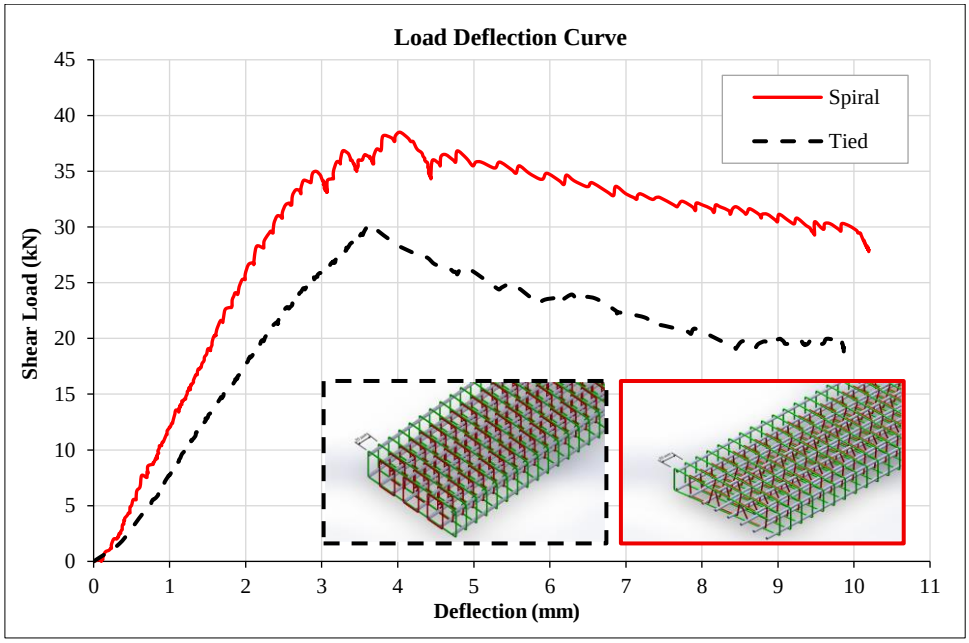

Figure 12. Load Versus Deflection Curve of Specimen with spacing (20 mm)

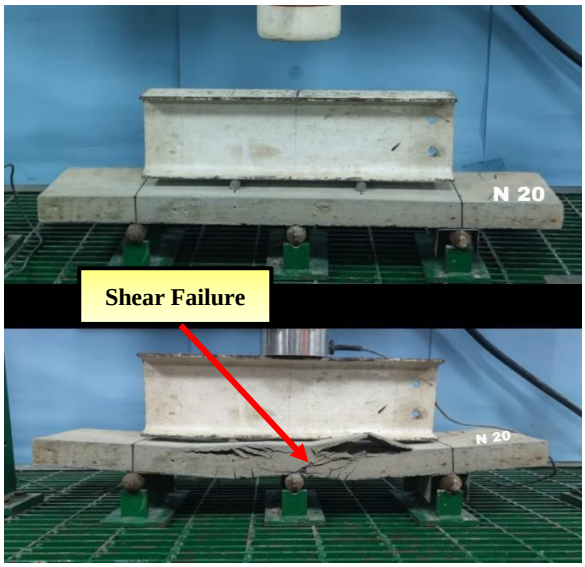

Figure 13. Loading of Specimen with Tied Stirrup Spacing (20 mm)

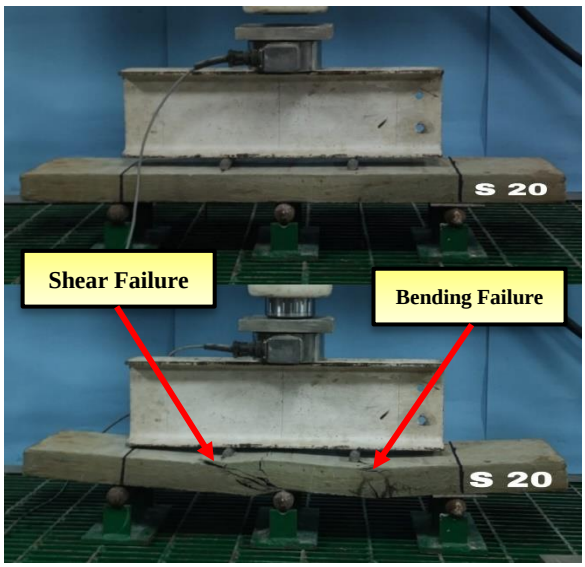

Figure 14. Loading of Specimen with Spiral Stirrup Spacing (20 mm)

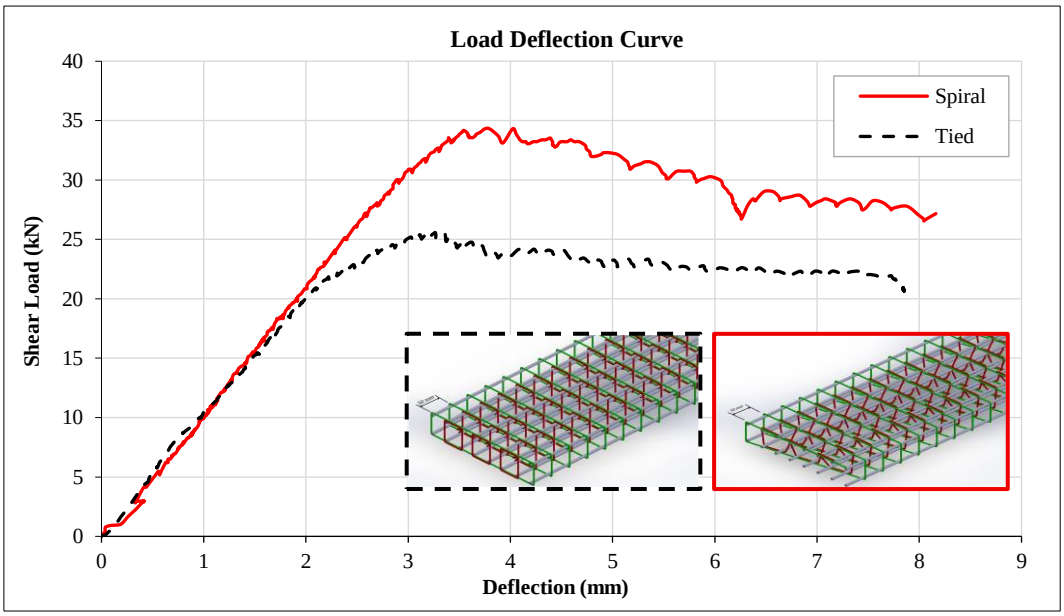

Figure 15. Load Versus Deflection Curve of Specimen with spacing (30 mm)

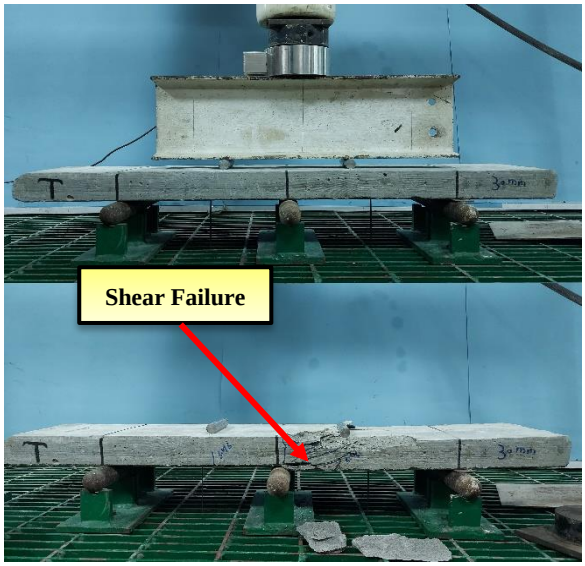

Figure 16. Loading of Specimen with Tied Stirrup Spacing (30mm)

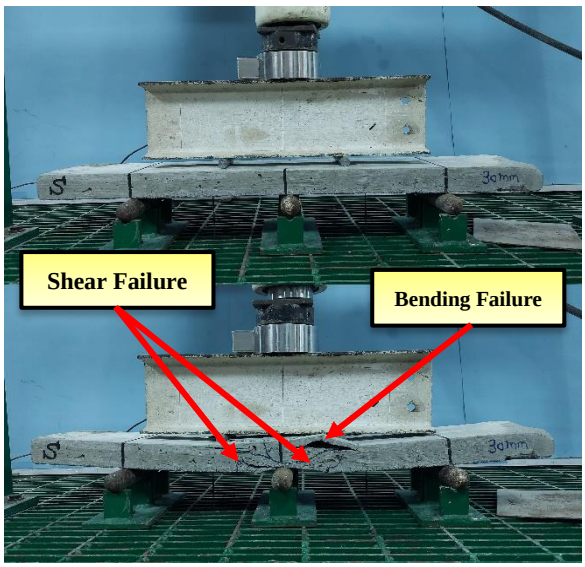

Figure 17. Loading of Specimen with Spiral Stirrup (30mm)

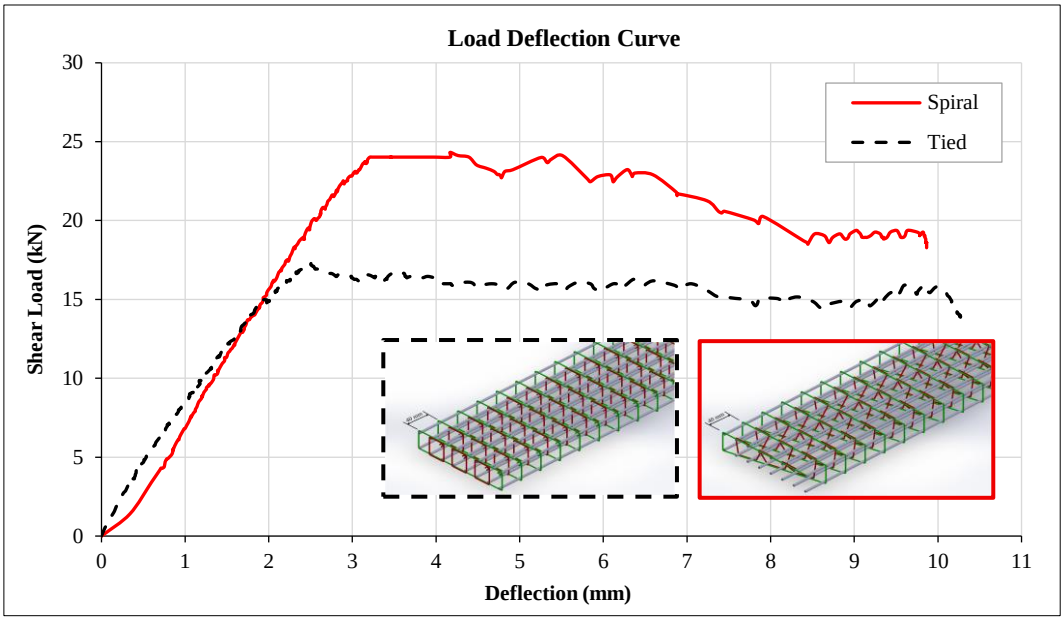

Figure 18. Load Versus Deflection Curve of Specimen with spacing (40 mm)

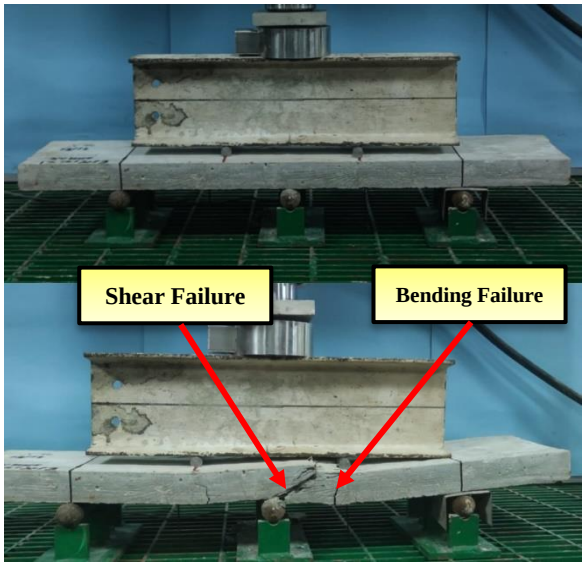

Figure 19. Loading of Specimen with Tied Stirrup Spacing (40 mm)

Figure 20. Loading of Specimen with Spiral Stirrup Spacing (40 mm)

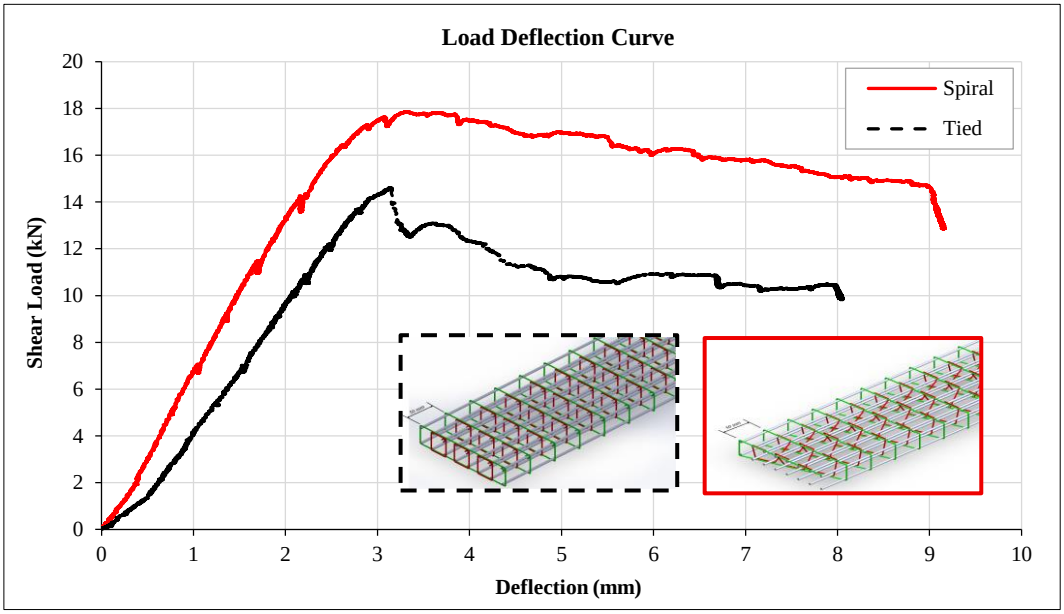

Figure 21. Load Versus Deflection Curve of Specimen with spacing (50 mm)

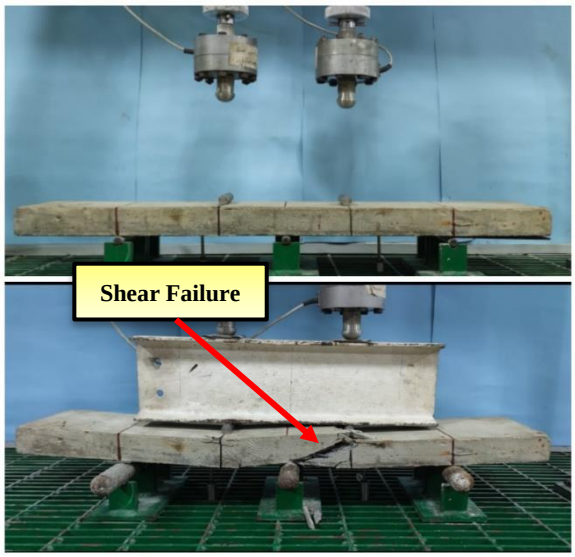

Figure 22. Loading of Specimen with Tied Stirrup Spacing (50 mm)

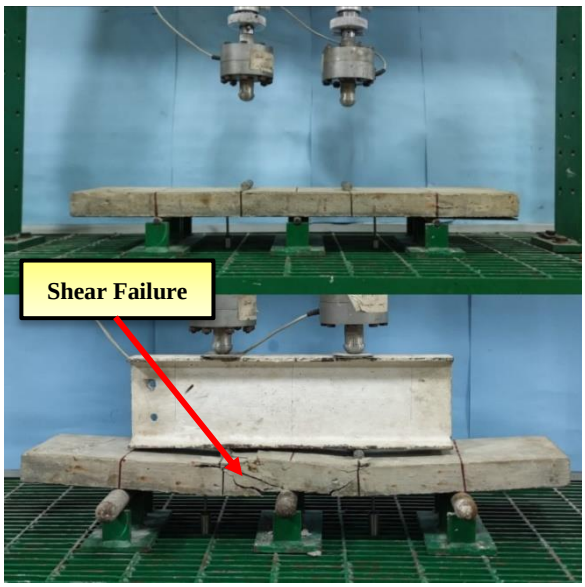

Figure 23. Loading of Specimen with Spiral Stirrup Spacing (50 mm)

The results indicate a clear trend that reducing stirrup spacing significantly improves shear performance. For example, at a 50 mm spacing, HB4 (specimen with normal stirrups) achieved a shear capacity of 14.61 kN with a peak deflection of 3.15 mm, whereas HB8 (specimen with spiral stirrups) reached 17.86 kN with a higher deflection of 3.31 mm. This demonstrates that staggered spiral stirrups not only increase the load-carrying capacity but also enhance post-cracking behavior. Closer spacing of spiral ties restricts the formation and propagation of diagonal shear cracks, thereby delaying failure and improving ductility. Prior to first cracking, all specimens exhibited nearly identical behavior, suggesting that initial elastic stiffness is largely governed by the longitudinal reinforcement and concrete characteristics. Beyond cracking, the load–deflection curves diverged, reflecting the contribution of transverse reinforcement in controlling crack width, redistributing stresses, and dissipating energy. Specimens with spiral stirrups showed a larger area under the curve, indicating superior energy absorption and enhanced deformation capacity.

The enhanced ductility observed in specimens with spiral reinforcement highlights the effectiveness of this configuration in improving structural performance. The use of continuous staggered spiral stirrups resulted in a notable improvement in shear performance. It was further observed that closer tie spacing significantly enhanced the ability of the reinforcement to restrict diagonal shear cracks and improve crack control. Although both configurations contributed to delaying shear failure, reduced spacing proved more effective in improving deformation capacity and overall shear resistance. Quantitatively, spiral reinforcement enhanced energy dissipation by approximately 46% compared to conventional stirrups.

The experimental findings underscore the potential for spiral reinforcement to reduce the amount of lateral reinforcement while achieving superior shear performance in hidden beams. Furthermore, the comparison between experimental results and calculated capacities based on international codes revealed that current design specifications tend to be conservative in predicting shear strength. This highlights the need to consider the contribution of spiral stirrups explicitly when evaluating shear capacity in design equations, which can lead to more efficient and economical structural solutions.

As observed in Figure 24, the type of lateral reinforcement had a significant impact on the load-carrying behavior of the hidden beams. Specifically, substituting conventional normal stirrups with staggered rectangular spiral stirrups increased the load capacity of specimens with normal stirrups by 22.24% and that of specimens without any stirrups by 27.29%. This improvement can be attributed to the spiral configuration's ability to better confine the concrete, control the propagation of diagonal shear cracks, and promote more uniform stress distribution throughout the beam. Furthermore, the ductility, represented by the area under the load–deflection curve, was strongly influenced by the type of transverse reinforcement. Specimens with spiral stirrups demonstrated a larger area under the curve, indicating higher energy absorption and the ability to undergo greater deformations prior to failure. These findings confirm that spiral reinforcement not only enhances shear strength but also substantially improves post-cracking behavior and overall structural performance, highlighting its potential as an effective alternative to conventional stirrups in hidden beam design.

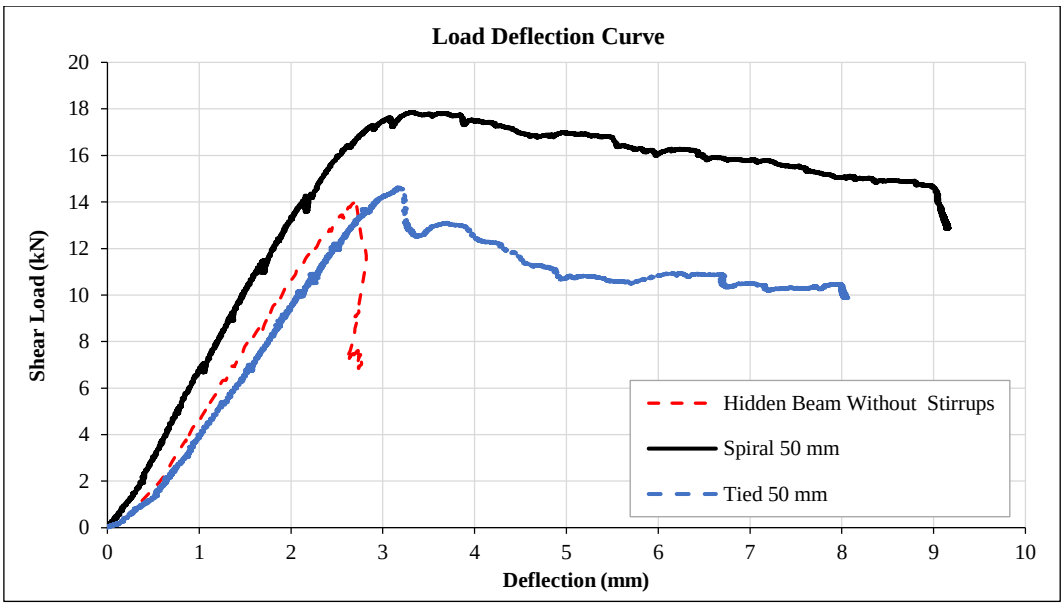

Figure 24. Load Versus Deflection Curve of Two Specimens (Beam of 50 mm spacing & Beam without Stirrups)

3.2. Cracking Propagation

Figures 25 to 27 illustrate the crack propagation at peak load for specimens with various stirrup configurations and spacings (HB1–HB9). In general, cracks near the midspan of all beams exhibited near-vertical orientations, while their angles gradually decreased as they approached the supports, reflecting the redistribution of shear stresses along the beam length. Specimen HB9, beam without stirrups, displayed a single prominent 45° diagonal crack at failure, consistent with the typical shear failure mechanism of beams without shear reinforcement. In contrast, specimens with lateral reinforcement exhibited more uniformly distributed cracks along their lengths, with spacing influenced by the type and arrangement of the stirrups. Compared to beams HB1, HB2, HB3, and HB4, beams HB5, HB6, HB7, and HB8 showed more cracks, indicating enhanced ductility and more gradual energy dissipation prior to failure. The load-deflection curves reflect the ductile behavior of the beams, which is demonstrated by the greater number of cracks. The smaller crack spacing in these specimens suggests that spiral reinforcement effectively confines the concrete and delays crack widening, promoting more uniform stress distribution. As the applied stress increased, a sequence of cracks parallel to the first crack was seen in the investigated beams. It was discovered that the distance between these cracks was less than that of specimens using normal stirrups. This observation suggests that implementing a spiral configuration for shear reinforcement effectively reduces the distance between cracks. The crack pattern exhibited by beam HB3 was not analogous to that of beam HB7; however, it was comparable to that of beam HB4. This finding suggests that the configuration of the shear reinforcement affects the crack pattern, and it is significantly influenced by the spiral pitch employed.

Figure 25. Cracking propagation of Normal stirrups for HB1, HB2, HB3, and HB4

Figure 26. Cracking propagation of staggered spiral for HB5, HB6, HB7, and HB8

Figure 27. Cracking propagation for specimen HB9, which has no stirrups

The first shear crack becomes noticeable at the mid-support of Specimen HB1 when a shear load of F = 14.49 kN is applied, with a spacing of 20 mm. These cracks extended in length up to F = 21 kN, but the crack width increased gradually. At F = 25.5 kN, the bar's slippage caused a negative flexural crack to form directly over the intermediate support. Eventually, it induced shear failure at a peak capacity of 30.18 kN, as shown in Figure 24. On the other hand, Figure 25 illustrates the crack propagation behavior associated with the use of spiral staggered ties. The first diagonal crack in HB5 appeared at 18.81 kN, growing gradually in length while the width increased more slowly. Shear cracks initiated within the shear zone at 28.5 kN and propagated upward at decreasing angles toward the loading points. Splitting occurred over the supports and extended into the compression zone, and the spiral stirrups yielded only at the peak load of 38.50 kN.

These observations indicate that both the number and configuration of transverse reinforcement significantly influence crack initiation, propagation, and failure patterns. Spiral reinforcement, due to its continuous and staggered arrangement, not only increases the number of cracks but also distributes them more evenly, reducing crack width and

delaying the onset of catastrophic failure. The results clearly demonstrate that closer spacing and spiral configurations enhance ductility, improve energy dissipation, and control crack growth more effectively than conventional stirrups. The findings also highlight that the spiral pitch is a key factor in determining crack morphology and propagation, emphasizing its importance in the design of hidden beams for optimal shear performance

3.3. Comparing the Results of the Present Study with Previous Studies

A comprehensive comparison between the present study and the previous studies of Elansary et al. (2021) [28], Youssef et al. (2024) [42], Abdullah et al. (2024) [24], and Chen et al. (2025) [27] underscores the distinct contributions of the proposed rectangular staggered spiral reinforcement system and clarifies the research gap addressed, as summarized in Table 4.

Table 4. Comprehensive comparison between the present study and the previous studies

Study	No. of Specimens	Beam Dimensions / Scale	Longitudinal Reinforcement	Transverse Reinforcement	Shear Capacity with respect to the reference beams	Crack Patterns / Failure Mode
Present Study	9 RC scaled-down hidden beams	Small-scale hidden beams, one-eighth scale	Identical longitudinal bars for all specimens (Top 8 ϕ 3 & Bottom 8 ϕ 4)	Rectangular, staggered, continuous spiral + conventional stirrups	Increased	Larger diagonal crack zones, reduced crack widths, and better crack distribution.
Elansary et al. (2021) [28]	6 RC beams + 18 cylinders	Wide full-scale RC beams	Identical longitudinal bars (Top 6 ϕ 18 & Bottom 10 ϕ 18)	Spiral lateral reinforcement (various configurations)	Increased	Cylinders: no cracks under splitting tension. Beams: a larger number of cracks with smaller spacing.
Youssef et al. (2024) [29]	22 miniature RC beams	one-eighth scale miniature RC beams	Identical longitudinal bars for all specimens (Top 2 ϕ 3 & Bottom 6 ϕ 4)	Staggered continuous spiral ties; normal ties for comparison	Increased	Larger diagonal cracks with spirals. Conventional ties showed localized cracks.
Abdullah et al. (2024) [24]	3 RC beams	Full-scale non-wide RC beams	For case 1-3 (4 D 10 T & 4 D 25 B) For case 2 (5 D 10 T & 5 D 25 B)	Vertical stirrup legs + conventional close stirrups	Increased	Smaller crack widths and density with more legs.
Chen et al. (2025) [27]	4 reinforced circular concrete members	Full-scale reinforced circular concrete members	Twelve GFRP bars with a nominal diameter of 12 mm	GFRP spiral grid vs. hoop stirrups	Increased	Spiral grid limited shear crack development.

Elansary et al. (2021) [28] primarily examined the confinement efficiency of circular spiral reinforcement in concrete cylinders and its subsequent influence on beam shear performance. Their findings revealed that the average compressive strength of the spirally confined cylinders was larger than that of the unconfined cylinders by 123, 110, and 120% for the cylinders with one, two, and three spirals, respectively. The same trend was observed for tensile strength with percentages of 250, 215, and 217%, respectively. When applied to beams, the spirally reinforced specimen (SP2-S100) achieved a failure load comparable to the reference beam while employing 47% less shear reinforcement, whereas other spiral configurations failed at loads 9–14% lower.

In contrast, the present study demonstrates consistently higher improvements in shear capacity. Beams reinforced with rectangular staggered spirals exhibited increases of 174%, 144%, 73%, and 27% relative to the reference beam without transverse reinforcement, surpassing the beam-level gains reported by Elansary et al. [28] Moreover, while Elansary et al. [28] primarily focused on load-carrying capacity, the present study provides a more detailed evaluation of structural behavior, including enhanced crack distribution, reduced crack width, improved confinement, and increased energy dissipation (46%). These results indicate that rectangular staggered continuous spirals are markedly more effective than conventional circular spirals for shear-critical hidden beams.

Similarly, Youssef et al. (2024) [42] examined the behavior of scaled beams with staggered spiral ties at 30 mm and 40 mm spacing. The results indicated increases in shear capacity of 33% and 27%, respectively, compared to conventional ties. Additionally, spiral ties contributed to larger diagonal crack zones and reduced crack widths, highlighting the role of continuous spirals in providing additional confinement and modifying crack patterns.

Abdullah et al. (2024) [24] studied the effect of multiple vertical stirrup legs on shear behavior in RC beams. The research demonstrated that increasing the number of vertical stirrup legs improved internal crack distribution and reduced crack widths. Normalized shear strength showed marginal increases, and the arrangement of stirrup legs influenced the initiation and propagation of diagonal cracks. This work highlighted the three-dimensional effects of stirrup placement on shear performance.

Chen et al. (2025) [27] investigated the shear performance of circular concrete members reinforced with an innovative fiber-reinforced polymer (FRP) stirrup. The study examined the effects of stirrup type and ratio on shear behavior. Results showed that FRP grid spiral-reinforced concrete cylinders (FSRCC) exhibited 16.2% higher shear strength than FRP hoop-reinforced cylinders (FHRCC), with failure mode shifting from shear tension to flexure compression. Increasing the stirrup ratio from 0.32% to 0.72% led to a maximum shear strength increase of 26.0%. The CSA S806–12 code accurately predicted FSRCC shear strength. A finite element model in ABAQUS/Explicit incorporating FRP–concrete bond-slip behavior simulated the shear response, and parametric analysis indicated that the longitudinal reinforcement ratio was the most influential factor for enhancing shear capacity. When the longitudinal reinforcement ratio increased from 0.9% to 3.4%, it showed a 118.3% improvement in ultimate shear strength.

Overall, the present study examines the influence of transverse reinforcement on the shear behavior of reinforced concrete (RC) beams, focusing on hidden beams and rectangular staggered continuous spirals. While previous research has shown that various transverse systems such as circular spirals, vertical stirrups, and grid spirals enhance shear capacity, control cracking, and improve ductility, the mechanical effects of staggered spirals in beams with reduced effective depth remain underexplored. This work addresses these gaps by evaluating multiple spacing configurations and providing quantitative data on crack patterns and energy absorption, offering a more comprehensive understanding of transverse reinforcement in shear-critical RC members

4. Analytical Predictions

The maximum load observed, Pmax, corresponds to the extreme shear strength, expressed as Vu = 0.30×Pmax at mid-support, the shear stress, which is calculated using the equation $v = Vu/bd$, and the deformation corresponding to the maximum recorded load during the test are all recorded. The shear strength is estimated using a range of code formulae, including the ACI Building Code, Eurocode 2, Japanese standard specifications, British Standards, and the standards outlined by the Canadian Standards. Table 5 summarizes the test results for miniature and equivalent prototype beams labeled HB1 through HB9. Table 6 presents a comparative analysis of the prototype results alongside calculated estimations based on ECP 2020, Eurocode 2, and ACI 318 for specimens HB1 to HB9. Additionally, Table 7 illustrates a comparison of the prototype results with calculated estimations derived from JSCE-2007, CSA-2004, and BS-8110 for the identical specimens.

Table 5. Test Results for miniatures and prototypes

Specimen	Results for miniatures		Results for prototype	
	Shear Capacity (KN)	Deflection at max load (mm)	Shear Capacity (KN)	Deflection at max load (mm)
HB1-N20	30.18	3.60	978.34	28.80
HB2-N30	25.57	3.27	828.89	26.16
HB3-N40	17.29	2.50	560.48	20.00
HB4-N50	14.61	3.15	473.61	25.20
HB5-S20	38.50	4.02	1248.04	32.16
HB6-S30	34.29	4.05	1111.57	32.40
HB7-S40	24.32	4.10	788.37	32.80
HB8-S50	17.86	3.31	578.96	26.48
HB9-No	14.03	1.88	454.81	15.04

Table 6. Comparative analysis of the prototype results and the calculated estimations based on ECP2020, ACI-318, and Eurocode-2

Specimen	Test results	ECP 2020		Eurocode-2		ACI-318	
	$V_{u,EXP}$	$V_{u,ECP}$	$V_{u,EXP}/V_{u,ECP}$	$V_{u,EC2}$	$V_{u,EXP}/V_{u,EC2}$	$V_{u,ACI}$	$V_{u,EXP}/V_{u,ACI}$
HB1-N20	2.40	1.00	2.40	1.32	1.818	1.40	1.714
HB2-N30	2.04	0.87	2.344	1.15	1.774	1.25	1.632
HB3-N40	1.38	0.81	1.703	1.07	1.289	1.18	1.169
HB4-N50	1.16	0.77	1.506	1.03	1.126	1.14	1.017
HB5-S20	3.07	1.00	3.07	1.32	2.325	1.40	2.192
HB6-S30	2.73	0.87	3.138	1.15	2.373	1.25	2.184
HB7-S40	1.94	0.81	2.395	1.07	1.813	1.18	1.644
HB8-S50	1.42	0.77	1.844	1.03	1.378	1.14	1.245
HB9-No	1.12	0.60	1.867	0.84	1.333	0.96	1.167

Table 7. Comparative analysis of the prototype results and the calculated estimations based on ECP2020, ACI-318, and Eurocode-2

Specimen	Test results	JSCE-2007		CSA-2004		BS-8110	
	$V_{u,EXP}$	$V_{u,JSCE}$	$V_{u,EXP}/V_{u,JSCE}$	$V_{u,CSA}$	$V_{u,EXP}/V_{u,CSA}$	$V_{u,BS}$	$V_{u,EXP}/V_{u,BS}$
HB1-N20	2.40	1.34	1.791	1.39	1.726	1.21	1.983
HB2-N30	2.04	1.16	1.758	1.25	1.632	1.07	1.906
HB3-N40	1.38	1.06	1.302	1.17	1.179	0.99	1.393
HB4-N50	1.16	1.01	1.148	1.13	1.026	0.95	1.221
HB5-S20	3.07	1.34	2.291	1.39	2.208	1.21	2.537
HB6-S30	2.73	1.16	2.353	1.25	2.184	1.07	2.551
HB7-S40	1.94	1.06	1,830	1.17	1.658	0.99	1.959
HB8-S50	1.42	1.01	1.406	1.13	1.256	0.95	1.494
HB9-No	1.12	0.78	1.435	0.96	1.167	0.78	1.436

4.1. Design Guidelines Provided by the ACI Building Code (ACI 318-02) [43]

In Equation 4 to 6, the shear strength is determined by calculating the average shear stress across the specified section defined by the width (b_w) and the effective depth (d). It is assumed that the shear is primarily supported by the concrete within the element, independent of any shear reinforcement (RFT). The overall shear strength is comprised of two components: a portion that is contributed by the concrete itself (V_c) and another that is provided by the shear reinforcement (V_s).

$$V_n = V_c + V_s \tag{4}$$

$$V_c = 0.17\lambda\sqrt{f_c'}b_w d \tag{5}$$

$$V_s = A_v f_{yv}\, d/s \tag{6}$$

where: V_n represents the overall nominal shear strength, while V_s and V_c designate the nominal shear strength contributions from stirrups and concrete, respectively. The modification factor λ equals 1 for normal-weight concrete. The stirrup area, yield stress, effective beam depth, and stirrup spacing are designated by A_v, f_{yv}, d, and s, respectively.

4.2. Design Guidelines Provided by the Eurocode (EC2-04) [44]

The Eurocode formula integrates the effects of shear reinforcement and concrete characteristics on shear resistance, demonstrating how concrete contributes to the overall capacity of the beam. The shear capacity, as defined by EC2 2004, is expressed through Equation 7 to 10. Within this context, the design shear strength of the concrete is represented by $V_{Rd,c}$, the design shear force resulting from the shear RFT is represented by $V_{Rd,s}$ and $V_{Rd,max}$ denotes the maximum shear force the specimen can withstand. The design shear force produced by external loads is represented by V_{Ed}. Furthermore, α indicates the angle between the VL ties and the beam axis, while ɵ represents the angle of the strut concerning the beam axis, perpendicular to the applied load. A_{sw} refers to the area of the shear RFT, S denotes the spacing of the stirrups, Fy is the yield strength of the shear RFT, and v1 is the strength reduction factor applicable to concrete that is cracked in shear conditions. If the relationship $V_{Ed} \leq V_{Rd,c}$ If it is satisfied, there is no need to calculate additional shear reinforcement. However, if $V_{Ed} > V_{Rd,c}$ it becomes essential to provide adequate shear reinforcement to ensure compliance with the condition $V_{Ed} \leq V_{Rd,c}$.

$$V_{Rd} = V_{Rd,c} + V_{Rd,s} \tag{7}$$

$$V_{Rd,c} = [C_{Rd,c}\ \mathrm{k}\ (100\,\rho_l\, f_{ck})^{1/3}\ ]\ \mathrm{bd} \tag{8}$$

$$V_{Rd,s} = \frac{A_{sw}}{S}\, \mathrm{z}\, f_{ywd}\, [\cot ɵ + \cot \alpha] \sin \alpha \tag{9}$$

$$V_{Rd,max} = [\frac{\alpha_{cw}\, b_w\, v1\, f_{cd}}{[\cot ɵ + \tan ɵ]}]\ 0.9\mathrm{d} \tag{10}$$

$\mathrm{K} = 1+\sqrt{\frac{200}{d}} \leq 2$, $C_{Rd,c} = 0.18/\gamma_c$, z = 0.9d, $\rho_l = \frac{Asl}{bd}$

4.3. Japan Standard Specifications (JSCE-2007) [45]

Equation 12 is applied to determine the shear capacity of design elements when shear reinforcement (RFT) is absent. In scenarios where longitudinal reinforcement and shear ties are present as shear RFT, the design shear capacity of an

element can be calculated using Equation 10. It is important to guarantee that the shear ties sustain at least 50% of the shear force provided by the shear RFT. In this context, α denotes the angle between the vertical shear ties and the beam axis, A_{sw} signifies the area of shear reinforcement, S represents the spacing between the shear ties, and f_{ywd} indicates the yield strength of the shear reinforcement.

$$V = V_{cd} + V_{sd} \quad (11)$$

$$V_{cd} = (\sqrt[4]{\frac{1000}{d}})(\sqrt[3]{100 * \frac{A_s}{bd}})(0.2\sqrt[3]{f_{cd}}).b_w.\frac{d}{1.3} \quad (12)$$

$$V_{sd} = [\frac{A_w f_{ywd}(\sin\alpha_s+\cos\alpha_s)}{S_s}]. Z/_{1.1} \quad (13)$$

4.4. Design Provisions of British Standards (BS-8110) [46]

In BS 8110, the shear capacity of reinforced concrete beams is determined using a combination of equations that take into account the beam's dimensions, material strengths, reinforcement, and other factors;

$$V = V_c + V_s \quad (14)$$

$$V_c = \frac{0.79}{\gamma_m}(\frac{100A_s}{b_w d})^{\frac{1}{3}}(\frac{400}{d})^{\frac{1}{4}}(\frac{F_{cu}}{25})^{\frac{1}{3}} \quad (15)$$

$$V_s = A_v f_y d/s \quad (16)$$

γ_m: is the reduction safety factor; F_{cu}: Compressive strength of cube

4.5. Canadian Code Standard Specifications (CSA-2004) [47]

Equation 18 is applied to determine the shear capacity of design elements when shear reinforcement (RFT) is absent. In scenarios where longitudinal reinforcement and shear ties are present as shear RFT, the design shear capacity of an element can be calculated using Equation 19.

$$V = V_c + V_s \quad (17)$$

$$V_c = [\beta.\sqrt{f_c'}]\ bd \quad (18)$$

$$V_s = A_v.f_y.d.\cot\theta/s \quad (19)$$

In this context, β is the factor indicating the ability of diagonally cracked concrete to transmit tension; f_c' is the concrete cylinder's compressive strength after 28 days, A_v signifies the area of shear reinforcement, S represents the spacing between the shear ties, and f_{ywd} indicates the yield strength of the shear reinforcement, θ angle between the compression strut and the longitudinal axis; equal to 45°.

4.6. ECP 203-20 [48]

As per ECP 203, shear stress is transferred through both the concrete and the shear reinforcement. Meanwhile, ECP 203-2011 overlooks the effect of vertical stirrups on RC hidden beams. The allowable shear stress, denoted as q_{cu}, is given by the corresponding equation. ECP 203 provides the methodology for calculating shear stress induced by vertical loads. The shear stress resulting from vertical RFT is represented by the equation qsu, while the equation qu represents the shear stress due to direct shear.

$$q_{cu}(\text{cracked}) = 0.12\sqrt{\frac{f_{cu}}{\gamma_c}} \quad (20)$$

$$q_{su} = \frac{n.A_{str}\, fy_{str}/\gamma_s}{b.s} \quad (21)$$

$$q_u = q_{cu} + q_{su} \quad (22)$$

4.7. Scaling the Results from the Scaled-down Laboratory Model to the Full-scale Prototype

Data integration translates the results from scaled-down models into the behavior of full-scale prototypes. The established relationship between the model and prototype enables the interpretation of outcomes from the smaller model to predict the prototype's performance. Correlating data from the scaled-down model is the primary goal of this work to obtain full-scale design information. Additionally, this study clearly demonstrates the relationship between the large and small scales. The stress similarity of the steel has been preserved, with the model yield strength remaining intact. $f_{y_{model}} = 691\ N/mm^2$, in contrast to the prototype yield strength $f_{y_{prototype}} = 350\ N/mm^2$. Staggered continuous ties

offer the same structural performance as conventional tie methods, but with a reduced reinforcement volume. Structures develop both enhanced shear capacity and greater power dissipation when engineers reduce the spacing between stirrups. The wider impact area of staggered continuous spiral reinforcement alters the direction of crack propagation at its onset. Such deviations create larger areas of cracking, which slow crack development until the structure attains greater structural integrity. The equivalent prototype beam section has a yield strength of reinforcement, $f_{y_{prototype}}$ = 360 N/mm². The beam has a cross-sectional dimension of b × t = 1400 mm × 320 mm. The type of beam used is continuous, having a span of 2.00 meters. It is strengthened with 18 tensile bars, which are 22 mm in diameter (18 ϕ 22), and nine compressive bars of 12 mm in diameter (9 ϕ 12). The lateral confinement is provided in 8 mm diameter ties (ϕ8) with a yield strength of 240 N/mm². The characteristic compressive strength of concrete is *fcu* = 40 MPa. Figure 28 illustrates the relation of shear capacity with stirrup spacing, whereas Figure 29 illustrates the relation of maximum load deflection to stirrup spacing based on the Equation 22.

$$\frac{Load_{prototype}}{Load_{model}} = \frac{f_{y_{prototype}}}{f_{y_{model}}} \times Scale^2 \quad (23)$$

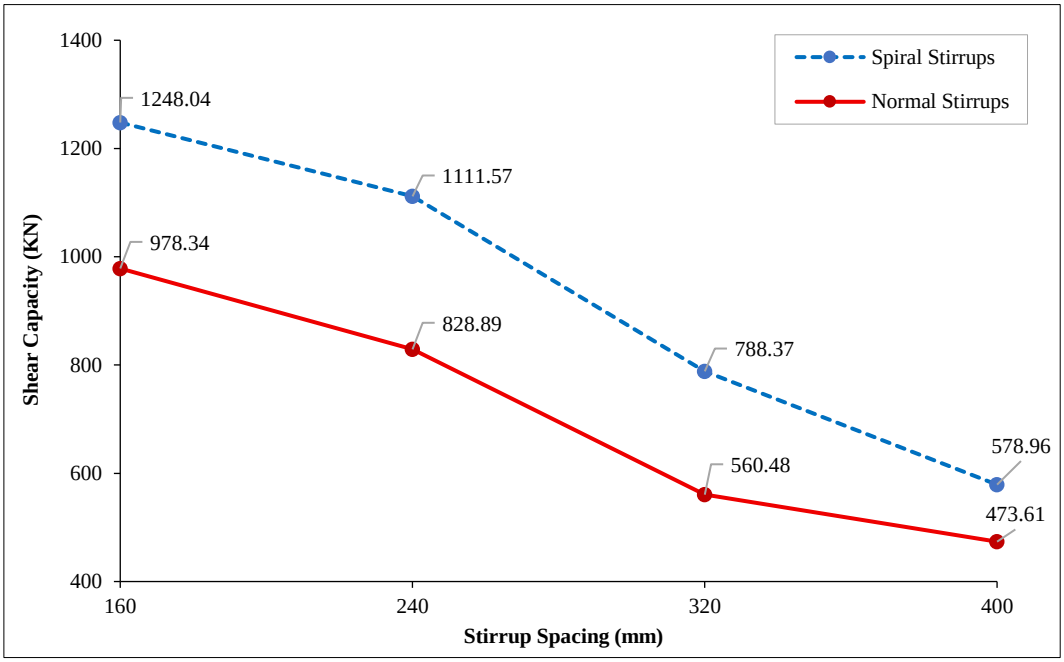

Figure 28. Shear capacity versus stirrup spacing for the prototype for spiral and regular stirrups

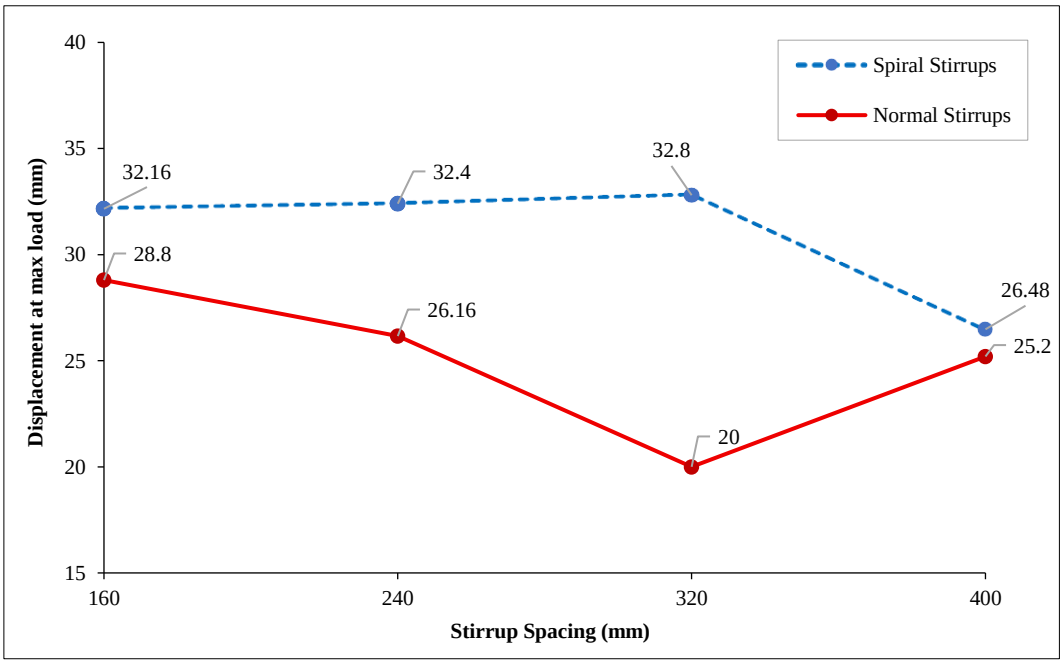

Figure 29. Displacement at max load versus stirrup spacing for the prototype for spiral and regular stirrups

4.8. Comparative Analysis between Experimental Results and the Numerical Predictions of Various Design Codes

Design code equations are inherently conservative due to the incorporation of safety factors. As observed in our study, various international standards, including JSCE 2015 [45], CSA A23.3 [47], ACI 318-02 [43], Eurocode, BS 8110 [46], and ECP 2020 [48], tend to underestimate the shear capacity of reinforced concrete (RC) beams with conventional transverse reinforcement. Figure 30 illustrates that the ultimate shear capacities predicted by these codes are slightly lower than the corresponding experimental values for beams with regular stirrups, reflecting the conservative nature of the design equations.

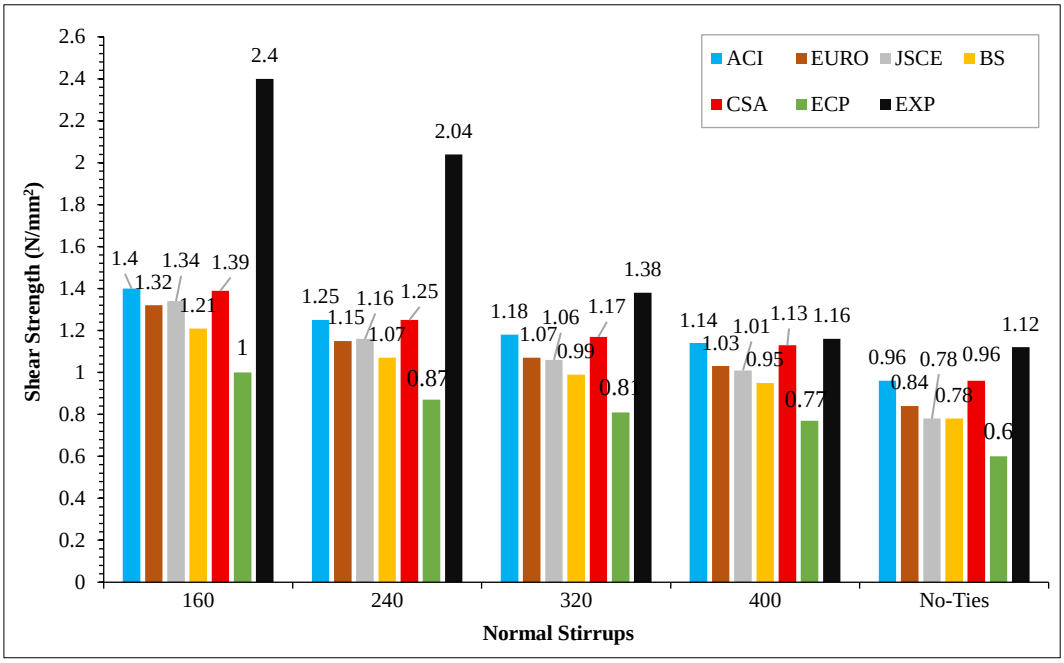

Figure 30. ACI318-02, Eurocode, JSCE, BS-8110, CSA, ECP2020, and experimental test results for normal stirrups

The disparity becomes more pronounced when evaluating beams with staggered spiral reinforcement. As shown in Figure 31, design codes significantly underestimate the shear capacity of these specimens, with calculated values much lower than experimental results. This difference arises primarily because most current code formulations do not account for the continuous and confining nature of spiral reinforcement, despite experimental evidence demonstrating its substantial contribution to shear resistance. Spiral stirrups improve stress redistribution, delay crack propagation, and enhance both ductility and energy absorption, effects that are not captured by conventional code predictions.

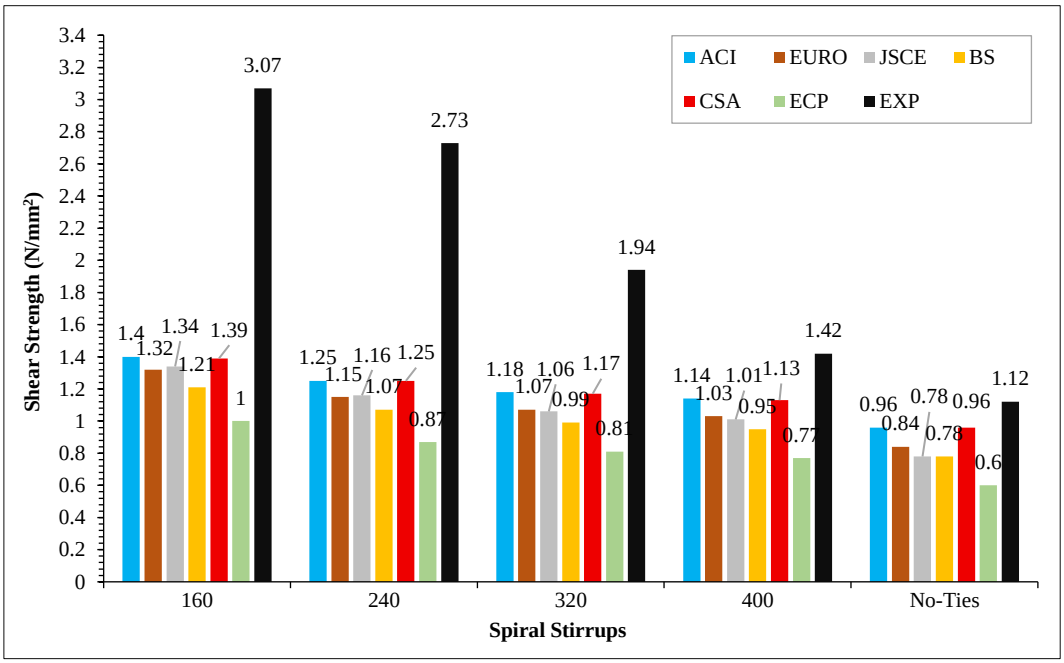

Figure 31. ACI318-02, Eurocode, JSCE, BS-8110, CSA, ECP2020, and experimental test results for spiral stirrups

The findings highlight the importance of explicitly accounting for the contribution of spiral reinforcement in shear capacity calculations to achieve more accurate and efficient designs. Furthermore, the experimental program utilized mortar instead of concrete to mitigate scale effects, ensuring that the observed improvements in shear performance can be reliably attributed to the reinforcement configuration rather than to size-dependent phenomena. These results underscore the potential for revising design codes to incorporate the benefits of continuous spiral reinforcement in hidden beams, leading to safer and more economical structural solutions.

5. Conclusions

Specimens reinforced with a combination of conventional ties and rectangular, staggered, continuous spiral ties were subjected to shear behavior analysis using a small-scale modeling approach. An experimental investigation was performed on nine small rectangular specimens with the same longitudinal reinforcement details. The shear tests were performed until the specimens failed. Finding out how well spiral ties work as internal transverse reinforcement to withstand shear tension was the main goal of this study. The analysis leads to the following conclusions:

- The use of staggered spiral ties was found to enhance the shear capacity and improve the overall shear performance of the tested beams.
- The presence of continuous spiral ties provides additional confinement, enhancing the compressive strength of concrete and consistently improving its capacity for shear transfer.
- The stress-strain relationships demonstrated that spirally reinforced beams exhibited enhanced ductility compared to unconfined beams, as indicated by a larger area under the load-deflection curves. This suggests greater energy absorption capacity and improved post-yield performance in the confined specimens.
- The spiral ties applied in reinforced specimens produced a larger zone of diagonal cracking as compared to the specimen containing regular ties, whose diagonal cracks were concentrated and localized.
- Spiral hooks significantly reduced the width of the cracks compared to regular ties, possibly due to their continuous spirals along the length of the beam, which allow for the easy bridging of cracks along the perimeter of the concrete.
- The beams reinforced with regular stirrups (HB1-N20, HB2-N30, HB3-N40, HB4-N50) recorded shear capacities higher than that of the reference beam (HB9-No, which had no transverse reinforcement) by 115%, 82%, 23%, and 4%, respectively. On the other hand, the same trend was observed for beams reinforced with spiral stirrups (HB1-S20, HB2-S30, HB3-S40, HB4-S50), which exhibited shear capacities that were also higher than the non-stirrup-reinforced reference beam by 174%, 144%, 73%, and 27%, respectively.
- Spiral confinement contributes to an increase in the shear load at the onset of shear cracking. The staggered spiral confinement contributes to the enhanced peak shear capacity, as indicated by experimental results.
- Based on these comparative analyses and study, it was found that the various reinforced concrete design codes—including the ECP-203, ACI-318, Eurocode, CSA-2004, JSCE-2007, and BS-8110 codes—tend to be highly conservative in estimating shear capacity. Furthermore, it was observed that wide (hidden) beams exhibit relatively higher safety factors compared to dropped (projected) beams.

The scope of this study was restricted to selected lateral reinforcement configurations characterized by specific spacing, bar diameters, and span-to-depth ratios. Therefore, additional experimental investigations encompassing a wider range of parameters and varied span-to-depth ratios are required to enhance the generalizability of the findings. Moreover, future research would benefit from a comparative evaluation of beams reinforced with conventional stirrups and those reinforced with spiral stirrups, provided that both configurations maintain an equivalent volume ratio of transverse reinforcement.

6. Abbreviations

As	Shear reinforcement cross sectional area	Asl	Area of tensile Rft
Ast	Stirrups cross sectional area	Av	Area of stirrups
b	Cross section width	d	Beam depth
E_s	Modulus of elasticity of steel	F_{cu}	Characteristic concrete strength
F_u	Ultimate stress of rebar	F_y	Yield stress of rebar reinforcement.
F_{ystr}	Yield stress of shear Rft.	LVDT	Load Variable Differential Transformers
P	Maximum applied load	$q_{cu\ cracked}$	Nominal shear strength of concrete for cracked sections
$q_{cu\ uncracked}$	Nominal shear strength of concrete for uncracked sections	$q_{u\ max}$	Maximum allowable shear stress regardless provided shear reinforcement
q_{su}	Shear stress provided by stirrups	q_u	Applied shear stress at critical section

Qu	Applied shear force at critical section	RC	Reinforced concrete
RFT	Reinforcement	S	Spacing between stirrups
V_c	Nominal shear strength provided by concrete	V_{cf}	Ratio between confined concrete volume to specimen total volume
V_{Ed}	Design shear force	V_n	Nominal shear strength
$V_{rd.c}$	Concrete shear resistance without shear Rft	$V_{rd.s}$	Shear resisted by stirrups
V_s	Nominal shear strength provided by stirrups	α	Inclination angle of stirrups with respect to longitudinal element axis
θf	Angle between concrete compression strut and beam axis	λ	Modification factor which equals to 1 for normal weight concrete
Φ	Diameter of steel bars	Ɛ	Strain
γ_c	Concrete partial safety factor	ACI	American Concrete Institute
ECP	Egyptian code practice	JSCE	Japan Society of Civil Engineers
RM	Reinforced mortar	SDM	Scale Down Modeling
HB1	Specimen 1 (Hidden beam with normal stirrups at spacing of 20 mm)	HB2	Specimen 2 (Hidden beam with normal stirrups at spacing of 30 mm)
HB3	Specimen 3 (Hidden beam with normal stirrups at spacing of 40 mm)	HB4	Specimen 4 (Hidden beam with normal stirrups at spacing of 50 mm)
HB5	Specimen 5 (Hidden beam with spiral stirrups at spacing of 20 mm)	HB6	Specimen 6 (Hidden beam with spiral stirrups at spacing of 30 mm)
HB7	Specimen 7 (Hidden beam with spiral stirrups at spacing of 40 mm)	HB8	Specimen 8 (Hidden beam with spiral stirrups at spacing of 50 mm)
HB9	Specimen 9 (Hidden beam with no stirrups)		

7. Declarations

7.1. Author Contributions

Conceptualization, M.A., J.J.E., A.Y., H.A., and A.M.; methodology, M.A.; validation, M.A., J.J.E., A.Y., H.A., and A.M.; formal analysis, M.A.; investigation, M.A.; resources, M.A., J.J.E., A.Y., H.A., and A.M.; data curation, J.J., A.Y., H.A., and A.M.; writing—original draft preparation, M.A.; writing—review and editing, M.A. and J.J.; visualization, J.J.E., A.Y., H.A., and A.M.; supervision, A.Y., H.A., and A.M.; project administration, M.A.; funding acquisition, J.J.E. All authors have read and agreed to the published version of the manuscript.

7.2. Data Availability Statement

The data presented in this study are available in the article.

7.3. Funding

This research is funded by the Indonesian Endowment Fund for Education (LPDP) on behalf of the Indonesian Ministry of Higher Education, Science and Technology and managed under the EQUITY Program (Contract No. 4299/B3/DT.03.08/2025 & No 3029/PKS/ITS/2025)) and Recognition as a World-Class University for Research Collaborations, IRN Type B1 year 2025 between Institut Teknologi Sepuluh Nopember and Cairo University.

7.4. Acknowledgments

The authors would like to express their sincere appreciation to the Concrete Laboratory and all its staff at the Structural Engineering Department, Faculty of Engineering, Cairo University, for providing full laboratory support and facilitating all required experimental work in the Miniature Models Laboratory.

7.5. Conflicts of Interest

The authors declare no conflict of interest.

8. References

[1] Meynagh, M. M., Yasouj, S. E. M., & Marsono, A. K. B. (2013). Reinforced Concrete Beam's Contribution on Sustainable Buildings. Engineering Research & Technology, 2(4), 138-143.

[2] Conforti, A., Minelli, F., Tinini, A., & Plizzari, G. A. (2015). Influence of polypropylene fibre reinforcement and width-to-effective depth ratio in wide-shallow beams. Engineering Structures, 88, 12–21. doi:10.1016/j.engstruct.2015.01.037.

[3] Mohammed, S. D., Salman, H. M., Ibrahim, T. H., Oukaili, N. K., & Allawi, A. A. (2025). On the Impact of Lacing Reinforcement Arrangement on Reinforced Concrete Deep Beams Performance. Civil Engineering Journal, 11(2), 726–745. doi:10.28991/CEJ-2025-011-02-019.

[4] Lubell, A. S., Bentz, E. C., & Collins, M. P. (2009). Shear reinforcement spacing in wide members. ACI Structural Journal, 106(2), 205–214. doi:10.14359/56359.

[5] Azimi, M., Bagherpourhamedani, A., Tahir, M. M., Sam, A. R. B. M., & Ma, C. K. (2016). Evaluation of new spiral shear reinforcement pattern for reinforced concrete joints subjected to cyclic loading. Advances in Structural Engineering, 19(5), 730–745. doi:10.1177/1369433216630371.

[6] Piscesa, B., Attard, M. M., Samani, A. K., & Tangaramvong, S. (2017). Plasticity constitutive model for stress-strain relationship of confined concrete. ACI Materials Journal, 114(2), 361–371. doi:10.14359/51689428.

[7] Shatarat, N., Katkhuda, H., Abdel-Jaber, M., & Alqam, M. (2016). Experimental investigation of reinforced concrete beams with spiral reinforcement in shear. Construction and Building Materials, 125, 585–594. doi:10.1016/j.conbuildmat.2016.08.070.

[8] Joshy, V., & Faisal, K. M. (2017). Experimental study on the behaviour of spirally reinforced SCC beams. International Journal of Engineering Research and General Science, 5(3), 96-105.

[9] Iyengar, K. T. S. R., Desayi, P., & Reddy, K. N. (1972). Confined concrete-Its application in R.C. beams and frames. Building Science, 7(2), 105–120. doi:10.1016/0007-3628(72)90047-3.

[10] Mander, J. B., Priestley, M. J. N., & Park, R. (1988). Theoretical Stress-Strain Model for Confined Concrete. Journal of Structural Engineering, 114(8), 1804–1826. doi:10.1061/(asce)0733-9445(1988)114:8(1804).

[11] Hu, B., & Wu, Y. F. (2018). Effect of shear span-to-depth ratio on shear strength components of RC beams. Engineering Structures, 168, 770–783. doi:10.1016/j.engstruct.2018.05.017.

[12] Meghana, M. B., & Vedic, N. (2018). Shear Capacity of RC Beams with Different Patterns of Spiral Reinforcements. International Journal of Engineering Research & Technology, 6(6), 2278–0181. doi:10.17577/IJERTCONV6IS06017.

[13] Kumar, T. R. S., & Sreevalli, I. Y. (2020). Numerical study on flexural performance of RC beam with various confinement pattern. Engineering Research Express, 2(1), 15016. doi:10.1088/2631-8695/ab68a3.

[14] Dewi, S. H., Thamrin, R., Zaidir, & Taufik. (2020). Effect of stirrup type on shear capacity of reinforced concrete members with circular cross section. E3S Web of Conferences, 156, 05022. doi:10.1051/e3sconf/202015605022.

[15] Karayannis, C. G., & Chalioris, C. E. (2013). Shear tests of reinforced concrete beams with continuous rectangular spiral reinforcement. Construction and Building Materials, 46, 86–97. doi:10.1016/j.conbuildmat.2013.04.023.

[16] Jaafar, K. (2008). Shear behaviour of reinforced concrete beams with confinement near plastic hinges. Magazine of Concrete Research, 60(9), 665–672. doi:10.1680/macr.2008.60.9.665.

[17] Jaafar, K. (2013). Utilising confinement reinforcement for shear resistance in reinforced concrete structures. Magazine of Concrete Research, 65(4), 220–233. doi:10.1680/macr.12.00061.

[18] Mohamed, H. A. (2018). Improvement in the Ductility of Over-reinforced NSC and HSC Beams by Confining the Compression Zone. Structures, 16, 129–136. doi:10.1016/j.istruc.2018.09.005.

[19] Tee, H. H., Al-Sanjery, K., & Chiang, J. C. L. (2018). Behaviour of over-reinforced concrete beams with double helix and double square confinements related to ultimate bending and shear strength. Journal of Physical Science, 29, 77–98. doi:10.21315/jps2018.29.s2.7.

[20] Abdelkhaliq, N. M., & Hilal, A. M. (2017). Experimental and Analytical Study of Confined Compression Zone on Capacity of Reinforced Concrete Beams. IOSR Journal of Mechanical and Civil Engineering, 14(01), 01–07. doi:10.9790/1684-1401070107.

[21] Li, W., Huang, W., Kong, Z., Fan, W., & Zhang, K. (2025). Shear behavior of SFRC beams reinforced with FRP stirrups: Experimental and analytical investigations. Steel and Composite Structures, 56(1), 83–98. doi:10.12989/scs.2025.56.1.083.

[22] Yu, Q., Yang, Y., Lin, Q., & Yang, D. (2024). Experimental Study on the Shear Behavior of HTRCS-Reinforced Concrete Beams. Buildings, 14(10), 3209. doi:10.3390/buildings14103209.

[23] He, J., Liu, J., Li, N., Li, J., & Fu, B. (2025). Shear behavior of concrete beams reinforced with GFRP-steel hybrid stirrups. Construction and Building Materials, 472, 140882. doi:10.1016/j.conbuildmat.2025.140882.

[24] Abdullah, M., Nakamura, H., & Miura, T. (2024). Experimental investigation on influence of vertical stirrup legs to shear failure behavior in RC beams. Developments in the Built Environment, 18. doi:10.1016/j.dibe.2024.100451.

[25] Ghalla, M., Bahrami, A., Mlybari, E., & Badawi, M. (2025). Shear behavior of reinforced concrete beams strengthened utilizing optimized external post-tensioning techniques. Frontiers of Structural and Civil Engineering, 19(6), 961–979. doi:10.1007/s11709-025-1185-4.

[26] Gouda, M. G., Mostafa, I. T., Mohamed, H. M., Sherif, A., & Agamy, M. H. (2025). Understanding the impact of spiral reinforcement on GFRP-RC beams under combined shear and torsion loading. Engineering Structures, 332, 120019. doi:10.1016/j.engstruct.2025.120019.

[27] Chen, C., Fang, H., Lim, Y. M., & Choo, B. (2025). Shear behavior of novel GFRP stirrup and GFRP bar reinforced circular concrete members. Engineering Structures, 345. doi:10.1016/j.engstruct.2025.121509.

[28] Elansary, A. A., Elnazlawy, Y. Y., & Abdalla, H. A. (2022). Shear behaviour of concrete wide beams with spiral lateral reinforcement. Australian Journal of Civil Engineering, 20(1), 174–194. doi:10.1080/14488353.2021.1942405.

[29] Youssef, A., Mawaad, S., & Salem, H. (2024). Shear capacity of miniature beams with continuous staggered spiral stirrups. Journal of Engineering and Applied Science, 71(1), 53. doi:10.1186/s44147-024-00380-3.

[30] Mahmoud, S., Youssef, A., & Salem, H. (2022). Enhanced Torsion Mechanism of Small-Scale Reinforced Concrete Beams with Spiral Transverse Reinforcement. Civil Engineering Journal (Iran), 8(11), 2640–2660. doi:10.28991/CEJ-2022-08-11-019.

[31] Elbasha, N. M., & Hadi, M. N. S. (2005). Effect of helical pitch and tensile reinforcement ratio on the concrete cover spalling off load and ductility of HSC beams. Proceedings of the Australian Structural Engineering Conference 2005, 2005, 54–64.

[32] Ziara, M. M., Haldane, D., & Hood, S. (2000). Proposed changes to flexural design in BS 8110 to allow over-reinforced sections to fail in a ductile manner. Magazine of Concrete Research, 52(6), 443–454. doi:10.1680/macr.2000.52.6.443.

[33] Mosley, W. H., Bungey, J., & Hulse, R. (1999). Reinforced Concrete Design Handbook. Palgrave Macmillan, London, United Kingdom.

[34] Ahmed, M. M., Farghal, O. A., Nagah, A. K., & Haridy, A. A. (2007). Effect of Confining Method on the Ductility of Over-Reinforced Concrete Beams. JES. Journal of Engineering Sciences, 35(3), 617–633. doi:10.21608/jesaun.2007.112873.

[35] Priastiwi, Y. A., Imran, I., Nuroji, & Hidayat, A. (2014). Behavior of ductile beam with addition confinement in compression zone. Procedia Engineering, 95, 132–138. doi:10.1016/j.proeng.2014.12.172.

[36] Priastiwi, Y. A., Imran, I., & Nuroji. (2015). The effect of different shapes of confinement in compression zone on beam's ductility subjected to monotonic loading. Procedia Engineering, 125, 918–924. doi:10.1016/j.proeng.2015.11.098.

[37] Jang, I.-Y., Park, H.-G., Kim, Y.-G., Kim, S.-S., & Kim, J.-H. (2009). Flexural Behavior of High-Strength Concrete Beams Confined with Stirrups in Pure Bending Zone. International Journal of Concrete Structures and Materials, 3(1), 39–45. doi:10.4334/ijcsm.2009.3.1.039.

[38] Ahmed, A., Mohammed, A. M. Y., & Maekawa, K. (2021). Correlation of High Cycle Fatigue Behavior of Circular and Square Reinforced Concrete Columns Subjected to Shear Controlled Cyclic Loading. KSCE Journal of Civil Engineering, 25(5), 1755–1764. doi:10.1007/s12205-021-0850-y.

[39] Mohammed, A. M. Y., Ali, A. R. M., & Abdalla, H. A. (2021). Non-linear behavior of low strength RC beams strengthened with CFRP sheets. Civil Engineering Journal (Iran), 7(3), 518–530. doi:10.28991/cej-2021-03091670.

[40] Mohammed, A. M. Y., & Maekawa, K. (2012). Global and local impacts of soil confinement on RC pile nonlinearity. Journal of Advanced Concrete Technology, 10(11), 375–388. doi:10.3151/jact.10.375.

[41] Abdelaal, A., & Youssef, A. (2023). Experimental investigation on corroded and non-corroded RC tunnels under different loading conditions. Journal of Engineering and Applied Science, 70(1), 146. doi:10.1186/s44147-023-00306-5.

[42] Youssef, A., Hegazy, M., & Mostafa, H. (2023). Performance of Isolated Footing with Several Corrosion Levels under Axial Loading. Civil Engineering Journal (Iran), 9(6), 1437–1455. doi:10.28991/CEJ-2023-09-06-011.

[43] ACI 318-19. (2019). Building Code Requirements for Structural Concrete. American Concrete Institute (ACI), Farmington Hills. United States.

[44] EN 1992-2. (2015). Design of concrete structures - Part 1-1: General rules and rules for buildings. European Committee for Standardization, Brussels, Belgium.

[45] JSCE. (2007). Standard specifications for concrete structures. Japan Society of Civil Engineers (JSCE), Tokyo, Japan.

[46] BS 8110-1:1997. (1997). Structural use of concrete: Code of practice for design and construction (BS 8110-1:1997). British Standards Institution (BSI), London, United Kingdom.

[47] CSA A23.3-04. (2004). Design of concrete structures. Canadian Standards Association (CSA), Toronto, Canada.

[48] ECP 203. (2020). The Egyptian Code for Design and Construction of Concrete Structures. Housing and Building Research Center, Giza, Egypt.